nature communications

Article

https://doi.org/10.1038/s41467-024-53790-5

CYP5122A1 encodes an essential sterol C4-methyl oxidase in *Leishmania donovani* and determines the antileishmanial activity of antifungal azoles

Received: 19 July 2023

Accepted: 20 October 2024

Published online: 31 October 2024

Check for updates

Yiru Jin[1,8], Somrita Basu[2,8], Mei Feng[1,8], Yu Ning[2], Indeewara Munasinghe[3], Arline M. Joachim[4], Junan Li[5], Lingli Qin[1], Robert Madden[2], Hannah Burks[2], Philip Gao[6], Judy Qiju Wu[7], Salma Waheed Sheikh[2], April C. Joice[4], Chamani Perera[3], Karl A. Werbovetz[4], Kai Zhang[2] & Michael Zhuo Wang[1]

Visceral leishmaniasis is a life-threatening parasitic disease, but current antileishmanial drugs have severe drawbacks. Antifungal azoles inhibit the activity of cytochrome P450 (CYP) 51 enzymes which are responsible for removing the C14α-methyl group of lanosterol, a key step in ergosterol biosynthesis in *Leishmania*. However, they exhibit varying degrees of antileishmanial activities in culture, suggesting the existence of unrecognized molecular targets. Our previous study reveals that, in *Leishmania*, lanosterol undergoes parallel C4- and C14-demethylation to form 4α,14α-dimethylzymosterol and T-MAS, respectively. In the current study, CYP5122A1 is identified as a sterol C4-methyl oxidase that catalyzes the sequential oxidation of lanosterol to form C4-oxidation metabolites. CYP5122A1 is essential for both *L. donovani* promastigotes in culture and intracellular amastigotes in infected mice. CYP5122A1 overexpression results in growth delay, increased tolerance to stress, and altered expression of lipophosphoglycan and proteophosphoglycan. CYP5122A1 also helps to determine the antileishmanial effect of antifungal azoles in vitro. Dual inhibitors of CYP51 and CYP5122A1 possess superior antileishmanial activity against *L. donovani* promastigotes whereas CYP51-selective inhibitors have little effect on promastigote growth. Our findings uncover the critical biochemical and biological role of CYP5122A1 in *L. donovani* and provide an important foundation for developing new antileishmanial drugs by targeting both CYP enzymes.

Human leishmaniasis is a complex of diseases caused by protozoan parasites of the genus *Leishmania*. The *Leishmania* parasites exist in the form of replicative promastigotes in the midgut of female sand flies. During a sand fly's blood meal, the infective metacyclic promastigotes are injected into the host and then taken up by macrophages, where they transform into intracellular amastigotes that can survive, persist, and disseminate within the host[1–3]. The main clinical manifestations include cutaneous, mucocutaneous, and visceral leishmaniasis. Among them, visceral leishmaniasis (VL) is the most severe, affecting liver, spleen, and bone marrow, and is fatal in over 95% of cases if left

A full list of affiliations appears at the end of the paper. e-mail: michael.wang@ku.edu

untreated[4]. There are an estimated 50,000 to 90,000 new VL cases per year globally[4]. VL is caused by *Leishmania donovani* in East Africa and on the Indian subcontinent and by *Leishmania infantum* in Europe, North Africa, and Latin America[5].

To date, there is no human vaccine for VL[6]. Chemotherapeutic drugs are limited and have drawbacks such as toxicity, long treatment regimens, emerging resistance, and/or high cost[7]. Therefore, there is still an unmet medical need for safe and effective antileishmanial drugs. The sterol biosynthesis pathway in *Leishmania* has been reported as a potential antileishmanial drug target[8,9]. Sterols (e.g., cholesterol and ergosterol) are integral components of biological membranes for regulating membrane fluidity and permeability. In addition, studies have shown that the perturbation of the sterol composition in *Leishmania* spp. led to mitochondrion dysfunction, superoxide accumulation, hypersensitivity to heat, and/or attenuated virulence in mice[10–12]. Unlike mammalian cells that synthesize cholesterol, *Leishmania* parasites synthesize ergosterol and other ergostane-based sterols. Ergosterol biosynthesis begins with the removal of methyl groups at lanosterol C4 and C14 positions (Supplementary Fig. 1). The C14-demethylation of the sterol precursor lanosterol is mediated by the sterol C14α-demethylase (CYP51), which is essential to *L. donovani*[13], but not to *L. major*, a causative agent for cutaneous leishmaniasis (CL)[11]. Leishmanial CYP51 can be inhibited by antifungal azole drugs, a class of fungal CYP51 inhibitors, which results in the accumulation of C14-methylated sterol intermediates and the depletion of ergostane-based sterols[14]. However, antifungal azoles exhibited significantly different antileishmanial activities in vitro. For example, ketoconazole or itraconazole at 1 μg/mL inhibited the growth of multiple strains of *L. donovani* and *L. infantum* promastigotes (<20% growth compared with control) whereas fluconazole did not (>80% growth)[14]. Fenticonazole and tioconazole were able to eliminate the intracellular amastigotes of *L. infantum* with EC_{50} values of 2.9 ± 0.3 μM and 4.0 ± 0.2 μM, respectively, but voriconazole failed[15]. Miconazole and clotrimazole strongly inhibited the growth of intracellular *L. major* and *L. amazonensis* at submicromolar concentrations[16] and itraconazole and posaconazole were also active against promastigotes and intracellular amastigotes of *L. amazonensis* (EC_{50} between 0.08 and 2.74 μM)[17]. In contrast, fluconazole and voriconazole were ineffective against these intracellular parasites (<50% inhibition) at 10 μM[16]. These results suggest that there may be other molecular targets in play that determine the antileishmanial activity of antifungal azoles. Our previous study examined differential sterol profiles of azole-treated *L. donovani* promastigotes and proposed a branched ergosterol biosynthetic pathway in *Leishmania*[18]. Specifically, the C14- and C4-demethylation reactions of lanosterol occur in parallel rather than sequentially as in fungi and the inhibition of both reactions may be required for optimal antileishmanial effect. As such, identification and characterization of the enzyme(s) responsible for lanosterol C4-demethylation is of paramount importance to understand sterol biology in *Leishmania* and lay a foundation to discover effective antileishmanial treatments that target the sterol biosynthetic pathway.

In most eukaryotes, the O_2-dependent sterol C4 demethylation is catalyzed by three enzymes: a C4 sterol methyl oxidase that sequentially generates hydroxy, aldehyde and carboxylate intermediates, a C4 decarboxylase, and a 3-ketosterol reductase (ERG27)[19–21]. In yeast and vertebrates, the same C4 sterol methyl oxidase (ERG25) works on both C4 methyl groups, whereas plants have two distinct ERG25 homologs that oxidize 4,4-dimethylsterols and 4α-methylsterols, respectively[22]. To date, information regarding the identity and therapeutic implications of sterol C4-demethylase in *Leishmania* remains scarce, in sharp contrast to CYP51 which has been investigated biochemically, genetically and pharmacologically in *Leishmania* and related trypanosomatids[23–26].

CYP5122A1 is a recently identified cytochrome P450 (CYP) enzyme which is well conserved among trypanosomatids[27] (Supplementary Fig. 2). Its amino acid sequence is only 22% identical to the CYP51 sequence and hence they belong to different CYP families, i.e., family 5122 and 51, respectively. It was reported that a heterozygous deletion of the *CYP5122A1* gene impairs parasite growth, mitochondrial function, and infectivity, although a *CYP5122A1* null mutant was untenable[27]. In addition, it was suggested that CYP5122A1 could be involved in ergosterol biosynthesis in *Leishmania* as the ergosterol content was reduced by 70% in the heterozygous knockout parasites and partially restored by complementation of *CYP5122A1* through episomal expression[27]. Moreover, CYP5122A1 heterozygous knockout parasites were significantly more sensitive to ketoconazole than the wild-type *L. donovani* promastigotes, although the underlying mechanism remains unknown[28]. It is also not clear if CYP5122A1 catalyzes the C4-demethylation reaction as CYP51 does for the C14-demethylation.

In this study, an N-terminal truncated construct of *L. donovani* CYP5122A1 was cloned, heterologously expressed, purified, and spectrally characterized. By reconstituting the catalytic activity of CYP5122A1 in vitro, its biochemical function in ergosterol biosynthesis was elucidated. Additionally, the essentiality of CYP5122A1 was evaluated for both *L. donovani* promastigotes and amastigotes using a complementing episome-assisted knockout approach coupled with negative selection. The effects of CYP5122A1 on cell growth, differentiation, stress responses, and expression of surface glycoconjugates were also assessed. Lastly, the association between CYP5122A1 inhibition and antileishmanial activities of antifungal azoles was determined. These results support that CYP5122A1 acts as the bona fide sterol C4-methyl oxidase, is essential to *L. donovani*, and helps determine the antileishmanial activity of antifungal azoles.

Results

Purified CYP51 and CYP5122A1 exhibited characteristic spectral properties of a CYP enzyme

L. donovani CYP5122A1 and CYP51 have an N-terminal transmembrane domain anchored to the endoplasmic reticulum, which needs to be removed from the recombinant protein constructs to facilitate expression and purification. We tested several truncations of CYP5122A1, and the removal of the first 60 amino acids from the N-terminus yielded the best expression results. Recombinant CYP51 (removal of the first 31 amino acids from the N-terminus) was designed based on a previous study on the N-terminal truncated *L. infantum* CYP51[24]. After expression and chromatographic purification, recombinant CYP5122A1 and CYP51 were obtained at high purity as indicated by the SDS-PAGE result (Supplementary Fig. 3A-B). Subsequent Western blot analysis of CYP5122A1 (Supplementary Fig. 3C) showed that the recombinant protein had slightly lower molecular weight compared with the native proteins detected in *Leishmania* spp. because of the deletion of the transmembrane domain.

CYP enzymes have an iron-containing heme as a prosthetic group whose different oxidation states can be characterized using UV-Vis spectroscopy. Results of spectral analysis demonstrated that the two proteins possessed properties typical of a CYP enzyme. Purified CYP5122A1 and CYP51 were in the oxidized state and displayed the Soret peak at 420 nm and 419 nm, respectively (Supplementary Fig. 3D, E). Upon reduction with dithionite and binding to CO, both enzymes exhibited the Soret peak at around 450 nm and almost no absorption at 420 nm in the presence of lanosterol (insets of Supplementary Fig. 3D, E). This indicated that they existed in the catalytically active P450 form rather than the inactive P420 form.

In the natural context, a CYP enzyme requires two electrons during a catalytic cycle. The electrons are donated by the cofactor NADPH and transferred to the CYP sequentially by its redox partner, CPR. However, three putative CPRs (XP_003862234.1, XP_003864839.1, and XP_003864409.1; protein sequence identity ranges from 21% to 27% between them) have been reported in the *L. donovani* genome and only one (XP_003862234.1 or LDBPK_281350) was recently characterized[29]. Previously, a recombinant CPR from another trypanosomatid *T. brucei* (TbCPR) has been characterized for

its P450 reduction activity and used as a surrogate CPR to reconstitute catalytic activities of CYP enzymes from *Leishmania* and *T. cruzi*[24,30,31]. Here, in the presence of NADPH, TbCPR was able to transfer the first electron to leishmanial CYP5122A1 and CYP51, and the resulting reduced CO difference spectra (Supplementary Fig. 4) were similar to the ones reduced by sodium dithionite. Therefore, TbCPR may be used as a surrogate redox partner in place of the endogenous leishmanial CPR for studying the catalytic activities of the two leishmanial CYP enzymes, although exact biochemical roles of the three putative leishmanial CPRs warrant future investigations.

CYP5122A1 had binding specificity to C4-methylated sterols

When a substrate binds to the CYP enzyme, it displaces the distal H_2O ligand of the heme iron, converting the heme iron from the low-spin state to the high-spin state. Such binding mode is termed "type I binding" and will yield a UV-Vis difference spectrum with a peak at 390 nm and a trough at 420 nm[32]. This unique feature was employed for identifying potential substrates of CYP5122A1. Six intermediate sterols within the ergosterol biosynthetic pathway (lanosterol, 4,14-DMZ, FF-MAS, T-MAS, zymosterol, and 7-dehydrodesmosterol; Supplementary Fig. 1) were tested due to their same tetracyclic ring structure, only differing in the number of methyl groups at C4 and/or C14 positions. Among them, sterols with at least one C4-methyl group (lanosterol, 4,14-DMZ, FF-MAS, and T-MAS) showed type I binding to CYP5122A1 (Fig. 1A), regardless of whether the C14-methyl group is present (lanosterol and 4,14-DMZ) or absent (FF-MAS and T-MAS). Zymosterol and 7-dehydrodesmosterol, which have no C4- or C14-methyl group, did not induce any appreciable change in the difference binding spectrum (Fig. 1A). These results suggest that C4-methylated sterols like lanosterol, 4,14-DMZ, FF-MAS, and T-MAS may serve as substrates of CYP5122A1. In comparison, CYP51, which is known to act as a C14-demethylase, exhibited a binding specificity distinct from CYP5122A1 (Fig. 1B). Only sterols with a C14-methyl group (lanosterol and 4,14-DMZ) showed typical type I binding to CYP51, consistent with a previous report[24]. The C14-demethylated sterols (FF-MAS and T-MAS) did not elicit any change in their difference binding spectra. Interestingly, zymosterol and 7-dehydrodesmosterol, which lack both C4- and C14-methyl groups, produced an atypical difference binding spectrum with a peak at 411 nm and a trough at 431-432 nm (Fig. 1B), which differs from the typical binding spectral changes, i.e., type I, II and reverse type I (also called pseudo or modified type II)[33]. Similar atypical spectral changes were also observed for the binding of racemic and *S*-bicalutamide to CYP46A1 through the bridging water ligand[34]. This suggests that zymosterol and 7-dehydrodesmosterol can enter the binding pocket of CYP51, albeit is unable to dislodge the hexacoordinated water molecule.

CYP5122A1 acted to oxidize the C4-methyl group of sterols in *Leishmania*

Using TbCPR as the redox partner, the catalytic activities of CYP5122A1 and CYP51 were reconstituted in vitro with the addition of NADPH. Interestingly, the optimal reaction pH was pH 6.2-6.6 for both enzymes, rather than physiological pH (Supplementary Fig. 5). Metabolite profiles were analyzed by comparing LC-MS/MS chromatograms of the reactions in the presence and absence of NADPH. As expected, CYP51 catalyzed the C14-demethylation of lanosterol and 4,14-DMZ and converted them to FF-MAS and 4-methylzymosterol, respectively (Fig. 2A, B). The alcohol, aldehyde, and carboxylate/formyloxy[35] intermediate metabolites generated during the sequential oxidation were also detected. The LC-MS/MS MRM (multiple reaction monitoring) transitions used for monitoring the intermediate oxidation metabolites of lanosterol and 4,14-DMZ were: 425 > 109 and 411 > 109 (hydroxy), 423 > 109 and 409 > 109 (aldehyde), 439 > 109 and 397 > 95 (carboxylate/formyloxy), respectively, based on the dehydrated molecular ions and common fragment ions of sterols[18]. In contrast, no oxidation metabolites were detected in the reactions of FF-MAS and T-MAS with CYP51 (Fig. 2C, D). The MRM transitions used for monitoring the intermediate oxidation metabolites of FF-MAS and T-MAS were: 409 > 109 and 411 > 109 (hydroxy), 425 > 109 and 409 > 109 (aldehyde), 423 > 109 and 425 > 109 (carboxylate/formyloxy), respectively. In addition, zymosterol and 7-dehydrodesmosterol were oxidized by CYP51 to form hydroxylated metabolites, which were detected in the MRM transition of 383 > 95 and 381 > 109, respectively (Fig. 2E, F). This is consistent with the atypical difference binding spectra of CYP51 with zymosterol and 7-dehydrodesmosterol observed above, although the exact location of hydroxylation remains unknown, presumably on or near C14.

When compared to CYP51, CYP5122A1 clearly showed a different substrate specificity and formed oxidation metabolites of different identities. Sterols that exhibited type I binding spectral change with CYP5122A1 (i.e., lanosterol, 4,14-DMZ, FF-MAS, and T-MAS) were also metabolized by this enzyme, yielding a mixture of alcohol, aldehyde, and/or carboxylate/formyloxy metabolites of the corresponding sterol substrate (Fig. 2A-D), whereas none of the zymosterol or 7-dehydrodesmosterol oxidation metabolites was detected (Fig. 2E, F). Importantly, the oxidation metabolites of lanosterol formed by CYP5122A1 had different LC retention times from those formed by CYP51. For example, the alcohol metabolite formed by CYP5122A1 (peak **7** in Fig. 2A) was eluted at 9.6 min, whereas the alcohol metabolite formed by CYP51 (peak **3** in Fig. 2A) was eluted at 7.1 min. This indicates that CYP5122A1 did not catalyze the same C14 methyl oxidation as CYP51 did. In contrast to CYP51, CYP5122A1 converted FF-MAS and T-MAS (both are C4-dimethylated and C14-demethylated sterols) to their corresponding alcohol, aldehyde, and carboxylate/formyloxy metabolites (Fig. 2C, D). Additionally, it was observed that CYP5122A1 converted 4,14-DMZ (a C4α-monomethylated and C14-methylated sterol) to an alcohol metabolite, but no aldehyde or carboxylate/formyloxy metabolite was detected (Fig. 2B). This result, along with the weaker binding of 4,14-DMZ to CYP5122A1 (Fig. 1A), suggests that CYP5122A1 may not be the optimal enzyme to catalyze the second C4-demethylation reaction and other enzymes like leishmanial Erg25 may still play a role, which warrants future investigations. No oxidation metabolite formation was seen for zymosterol or 7-dehydrodesmosterol with CYP5122A1. As expected, NADPH was required for the catalytic activity of both CYP51 and CYP5122A1 (Fig. 2). Taken together, these findings prompted us to propose CYP5122A1 as a sterol C4-methyl oxidase or a sterol C4-demethylase, assuming that the carboxylate metabolites formed by CYP5122A1 will be decarboxylated and reduced by a dehydrogenase/decarboxylase and a 3-ketosterol reductase, respectively.

To fully elucidate the biochemical role of CYP5122A1, its reaction with lanosterol was scaled up from 0.1 mL to 770 mL so that sufficient amounts of oxidation metabolites could be isolated, purified, and analyzed by NMR spectroscopy for structural identification. The exact mass of the purified metabolite was 423.360 Da as the dehydrated molecular ion $[M+H-18]^{+1}$, which is within 7 ppm of the predicted exact mass (423.363 Da; $C_{30}H_{47}O$) of the proposed aldehyde metabolite. The 1D and 2D NMR spectra of the aldehyde metabolite (2.1 mg; referred to as "unknown") were successfully collected. The structure of the aldehyde metabolite was elucidated using comparison of its ^{1}H and ^{13}C NMR spectra with pre-assigned lanosterol standard (Fig. 3A, B and Supplementary Table 2 for selected ^{1}H and ^{13}C NMR signals), heteronuclear multiple bond correlation (HMBC; Supplementary Fig. 6A), heteronuclear single quantum coherence (HSQC; Supplementary Fig. 6B), and nuclear overhauser effect spectroscopy (NOESY; Supplementary Fig. 6C) 2D NMR. First, the presence of a singlet at 9.40 ppm in the unknown ^{1}H NMR spectrum (Fig. 3A) and a signal at 207.2 ppm in the unknown ^{13}C NMR spectrum (Fig. 3B) that were absent in the corresponding NMR spectra of the lanosterol standard clearly indicate the existence of the aldehyde group in the unknown molecule.

https://doi.org/10.1038/s41467-024-53790-5

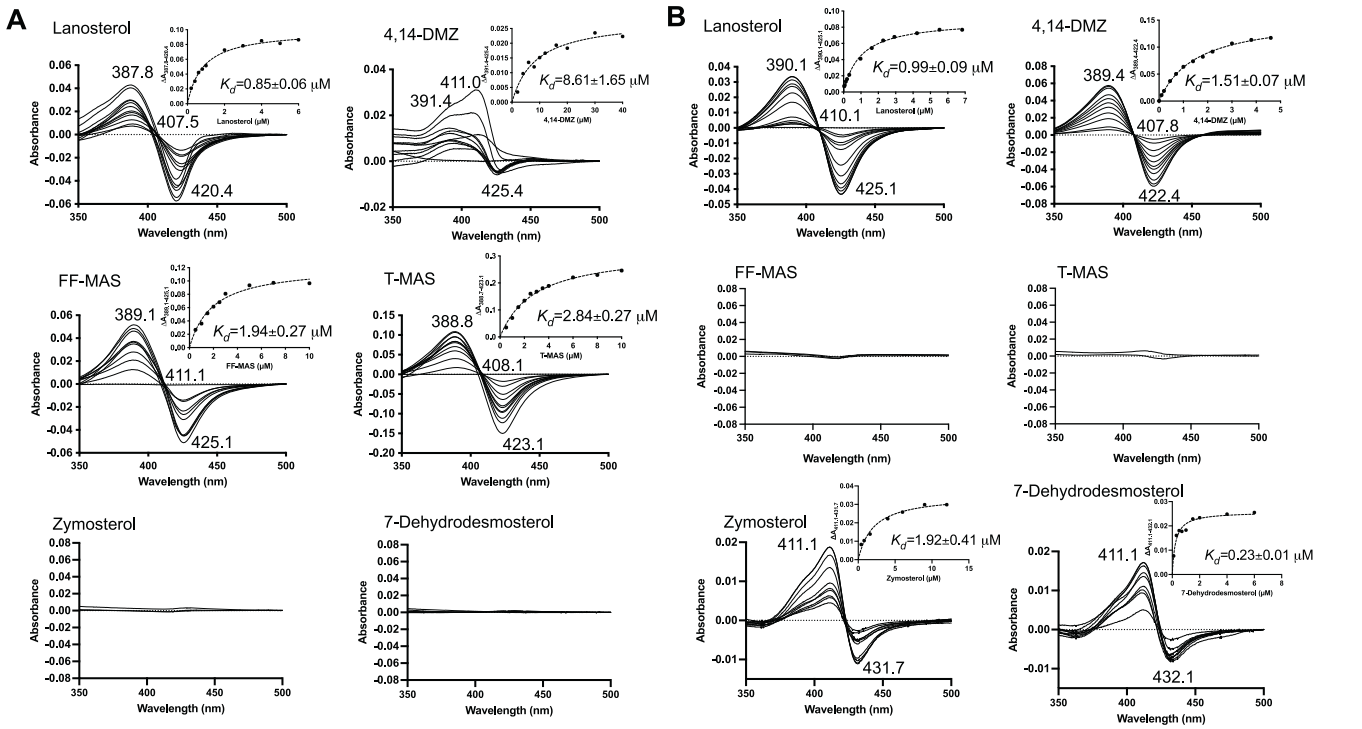

Fig. 1 | Binding spectra of sterols with CYP5122A1 and CYP51. Purified recombinant CYP5122A1 (**A**) and CYP51 (**B**) (in the oxidized ferric form) were incubated with an increasing amount of sterol ligands and difference spectra were recorded over a reference sample that only contained protein and buffer. Dissociation constant (K_d) was derived by fitting the equation $\Delta A = \Delta A_{max}[L]/(K_d + [L])$ to the peak-to-trough absorbance difference (ΔA) versus the ligand concentration ([L]) curve, where ΔA_{max} is the maximal amplitude of the spectral response.

Second, the location of this aldehyde group was revealed by the HMBC correlations between H-28 aldehyde proton (9.40 ppm) and C-4 carbon (55.4 ppm) (Supplementary Fig. 6A) and between C-28 aldehyde carbon (207.2 ppm) and multiple nearby proton signals, i.e., H-29 methyl (1.09 ppm), H-5 (1.61 ppm), and H-3 (3.79 ppm) (Supplementary Fig. 6A). The assignment of the H-29 methyl signal was confirmed by its HMBC correlations with C-3 (71.9 ppm), C-4 (55.4 ppm) and C-5 (43.7 ppm) (Supplementary Fig. 6A). The assignment of C-3 and C-5 was substantiated by the HSQC correlations between C-3 (71.9 ppm) and C-5 (43.7 ppm) with their corresponding protons H-3 (3.79 ppm) and H-5 (1.61 ppm) (Supplementary Fig. 6B). Moreover, the HSQC spectrum of the unknown showed correlation between the aldehyde carbon C-28 (207.2 ppm) and the aldehyde hydrogen H-28 (9.40 ppm) (Supplementary Fig. 6B). Third, when comparing ^{1}H NMR methyl signals of the unknown to those of lanosterol, all methyl signals were present except for H-28 methyl (1.00 ppm lanosterol) as shown by the dotted line in Fig. 3A. Methyl signals for H-18 (0.68 ppm, s), H-21 (0.91 ppm, d), H-26 (1.68 ppm, s), and H-27 (1.60 ppm, s) in the unknown compound exhibited chemical shifts identical to those in lanosterol (Fig. 3A and Supplementary Table 2). However, methyl signals for H-19 (1.03 vs. 0.98 ppm, s) and H-29 (1.09 vs. 0.81 ppm, s) shifted downfield (Fig. 3A and Supplementary Table 2), indicating the presence of a nearby electron-withdrawing group in the unknown, consistent with the presence of an aldehyde at C-4 position in the proposed structure of the unknown. This aldehyde group in the unknown also caused a downfield shift of C-4 signals (55.4 vs. 39.0 ppm; Fig. 3B and Supplementary Table 2). Fourth, the assignment of H-30 (0.88 ppm), H-19 (1.03 ppm), H-27 (1.60 ppm) and H-26 (1.68 ppm) signals were also confirmed by their HMBC correlations with the olefinic carbons C-24 (125.3 ppm), C-25 (131.2 ppm), C-9 (134.1 ppm) and C-8 (135.0 ppm) (Supplementary Fig. 6A). Lastly, it is noteworthy that the signal associated with H-30 methyl (0.88 ppm), which is connected to C-14, is present in both ^{1}H NMR spectra of lanosterol and the unknown compound (Fig. 3A and Supplementary Table 2). The assignment of H-30 can be further confirmed by HMBC correlation with olefinic C-8 carbon (135.0 ppm, Supplementary Fig. 6A). These NMR results strongly point towards a structure containing an aldehyde group that replaces one of the methyl groups at the C-4 position in lanosterol. The NOESY spectrum (Supplementary Fig. 6C) of the unknown shows through space interaction of H-28 (9.40 ppm) hydrogen with H-3 (3.79 ppm) and H-5 (1.61 ppm) hydrogens, indicating that the aldehyde group is projecting below the plane of the paper. It should be noted that not all the observed signals in the NMR spectra were contributed by the aldehyde metabolite. In the ^{1}H NMR spectrum (Fig. 3A), the broad peak at 1.26 ppm and the multiplet at 0.86 ppm (indicated by asterisks) were caused by the contamination of grease[36]. An impurity (indicated by hashtags in Fig. 3A, B) was present in both lanosterol standard and the unknown sample and it was partially elucidated as a sterol side chain oxidation product (Supplementary Fig. 7 and Supplementary Table 3). In the ^{13}C NMR spectrum (Fig. 3B), peak at 100 pm could not be assigned to the aldehyde metabolite due to the lack of any correlation in HMBC and HSQC spectra, supporting that this signal is not part of the molecule of interest. Taken together, these NMR spectroscopy and LC-MS/MS sterol analysis results unequivocally support that CYP5122A1 catalyzes the sequential oxidation reaction of the lanosterol C4 methyl groups, leading to C4-demethylation during ergosterol biosynthesis in *Leishmania*.

CYP5122A1 was essential for *L. donovani* promastigotes in culture

To assess the essentiality of *CYP5122A1*, we applied a complementing episome-assisted knockout approach coupled with negative selection (Supplementary Fig. 8A)[37]. Briefly, we first replaced one allele of the *CYP5122A1* gene with the BSD-resistance cassette to generate the Ld22A1 + /– mutant by homologous recombination. The heterozygotes (half knockout) were then episomally transfected with pXNG4-22A1

https://doi.org/10.1038/s41467-024-53790-5

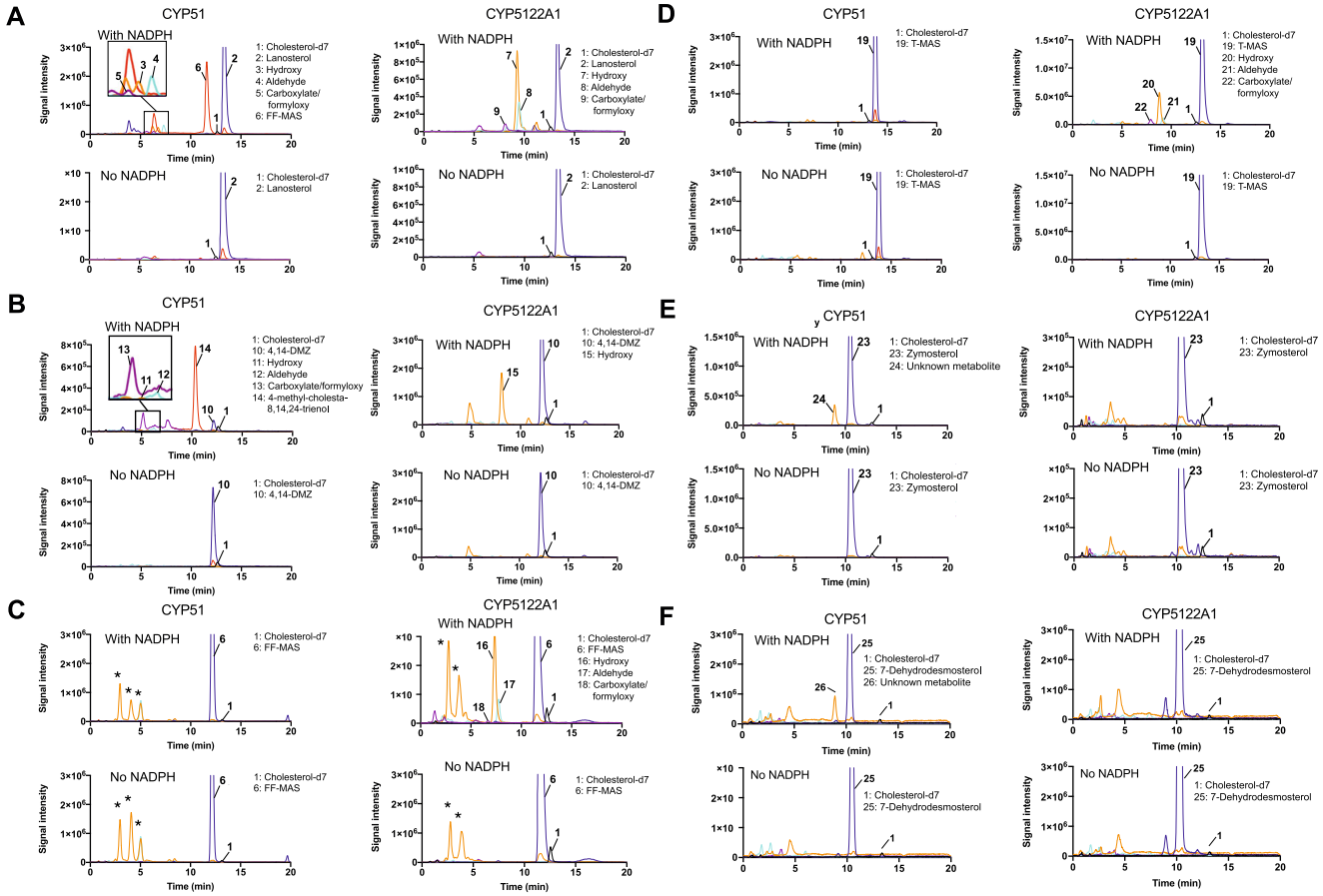

Fig. 2 | LC-MS/MS chromatograms of CYP reconstitution assays using various sterol substrates. Recombinant CYP5122A1 and CYP51 were reconstituted with (**A**) lanosterol, (**B**) 4,14-DMZ, (**C**) FF-MAS, (**D**) T-MAS, (**E**) zymosterol, and (**F**) 7-dehydrodesmosterol as the sterol substrates. The peaks of the internal standard cholesterol-d7 (black), substrates (blue), hydroxy metabolites (orange), aldehyde metabolites (cyan), carboxylate/formyloxy metabolites (purple), and 14-demethylated products (red) were indicated in the chromatograms. Peaks with asterisk were detected in both incubations with or without NADPH and hence considered as background signals.

carrying SAT, GFP, and TK, followed by the replacement of the second allele of *CYP5122A1* with the PAC-resistance cassette to generate the chromosomal null mutant Ld22A1^{-} + pXNG4-22A1 (Supplementary Fig. 8B, C). Promastigotes were able to proliferate in complete M199 medium after these genetic manipulations, though Ld22A1 + /– +pXNG4-22A1 and Ld22A1^{-} + pXNG4-22A1 exhibited delayed growth in vitro (Supplementary Fig. 9A). They attained the same plateau densities as Ld1S WT and Ld22A1 + /– on day 5 (one day later). The obtained mutants were assessed at the protein level by Western blot analysis (Supplementary Fig. 9B, C). Compared to Ld1S WT, Ld22A1 + /– showed a reduced level of CYP5122A1 ($p < 0.01$), whereas the heterozygous and null mutants transfected with pXNG4-22A1 had overexpression of CYP5122A1 ($p < 0.001$). Meanwhile, the genetic manipulation of *CYP5122A1* did not affect the CYP51 expression significantly (Supplementary Fig. 9B, C).

To determine if *CYP5122A1* is required for promastigotes, Ld22A1 + /– +pXNG4-22A1 and Ld22A1^{-} + pXNG4-22A1 (clone #1 and #2) were cultivated in the absence or presence of selective drugs (nourseothricin as the positive selection drug to retain pXNG4-22A1 and GCV as the negative selection drug to expel plasmid) and analyzed for GFP expression in each passage as a readout for plasmid retention (Fig. 4). When growing in media containing nourseothricin (SAT), all cell lines maintained high levels of GFP fluorescence (> 95% GFP-high) through multiple passages as expected (Fig. 4A, C). Without nourseothricin or GCV, the heterozygous mutant and clone #1 of the chromosomal-null mutant retained high levels of GFP, whereas the percentage of GFP-high population in clone #2 of the chromosomal-null mutant gradually decreased to ~30% after 17 passages. These findings allude to clonal variations among the *CYP5122A1* mutants in their ability to retain pXNG4-22A1 in the absence of selective pressure. When cultivated in the presence of GCV and absence of nourseothricin, cells would favor eliminating the plasmid to avoid toxicity if the plasmid did not contain any essential genes. Conversely, if there was an essential gene on the plasmid, cells would retain the plasmid despite the associated cost[37]. As shown in Fig. 4A, Ld22A1 + /– +pXNG4-22A1 promastigotes progressively lost their GFP expression to <5% GFP-high by passage 17 in GCV, indicating that pXNG4-22A1 was dispensable in this cell line which had one *CYP5122A1* endogenous allele. In comparison, GCV treatment lowered the percentage of GFP-high population in Ld22A1^{-} + pXNG4-22A1 to a much lesser extent (~58% and ~30% for clone #1 and #2, respectively; Fig. 4A, D). To examine if the plasmid was required for the survival and proliferation of Ld22A1^{-} + pXNG4-22A1, we separated GFP-high and GFP-low cells from Ld22A1^{-} + pXNG4-22A1 clone #2 grown in the presence of GCV (Fig. 4D) by FACS and then isolated two single clones of each population via serial dilution. Importantly, clones isolated from the GFP-low population (#2-1 and #2-2) quickly regained GFP expression after two rounds of amplification (+GCV, -SAT) (Fig. 4E, F). Southern blot analysis verified that clones from both GFP-high (#2-15 and #2-16) and GFP-low (#2-1 and #2-2) populations were still chromosomal null for *CYP5122A1* (Fig. 4G). Finally, Western blots revealed robust expression of CYP5122A1 in these sorted clones at levels similar to Ld22A1 + /- +pXNG4-22A1 and

https://doi.org/10.1038/s41467-024-53790-5

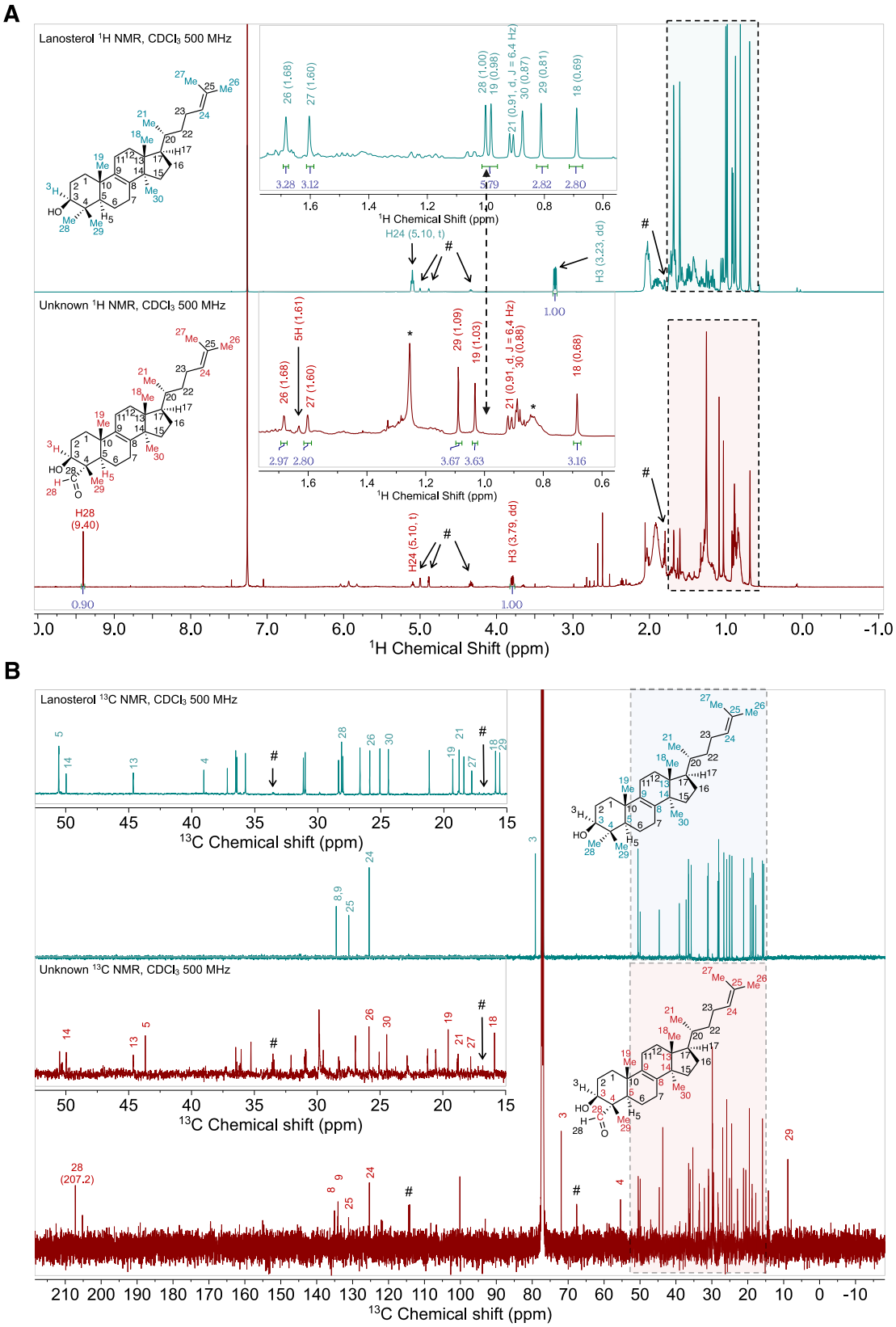

Fig. 3 | 1D NMR spectra of the purified metabolite (unknown) of lanosterol from incubations with CYP5122A1. 1H (**A**) and 13 C (**B**) NMR spectral comparison between lanosterol (reference) and the purified metabolite indicating the presence of the aldehyde group in the purified metabolite. Hashtags (#) indicate signals of an impurity present in both the lanosterol standard and the unknown sample (see Supplementary Fig. 7 and Supplementary Table 3 for chemical shifts and proposed partial structure of this impurity). Asterisks (*) indicate signals of grease contamination (broad peak at 1.26 ppm and the multiplet at 0.86 ppm).

https://doi.org/10.1038/s41467-024-53790-5

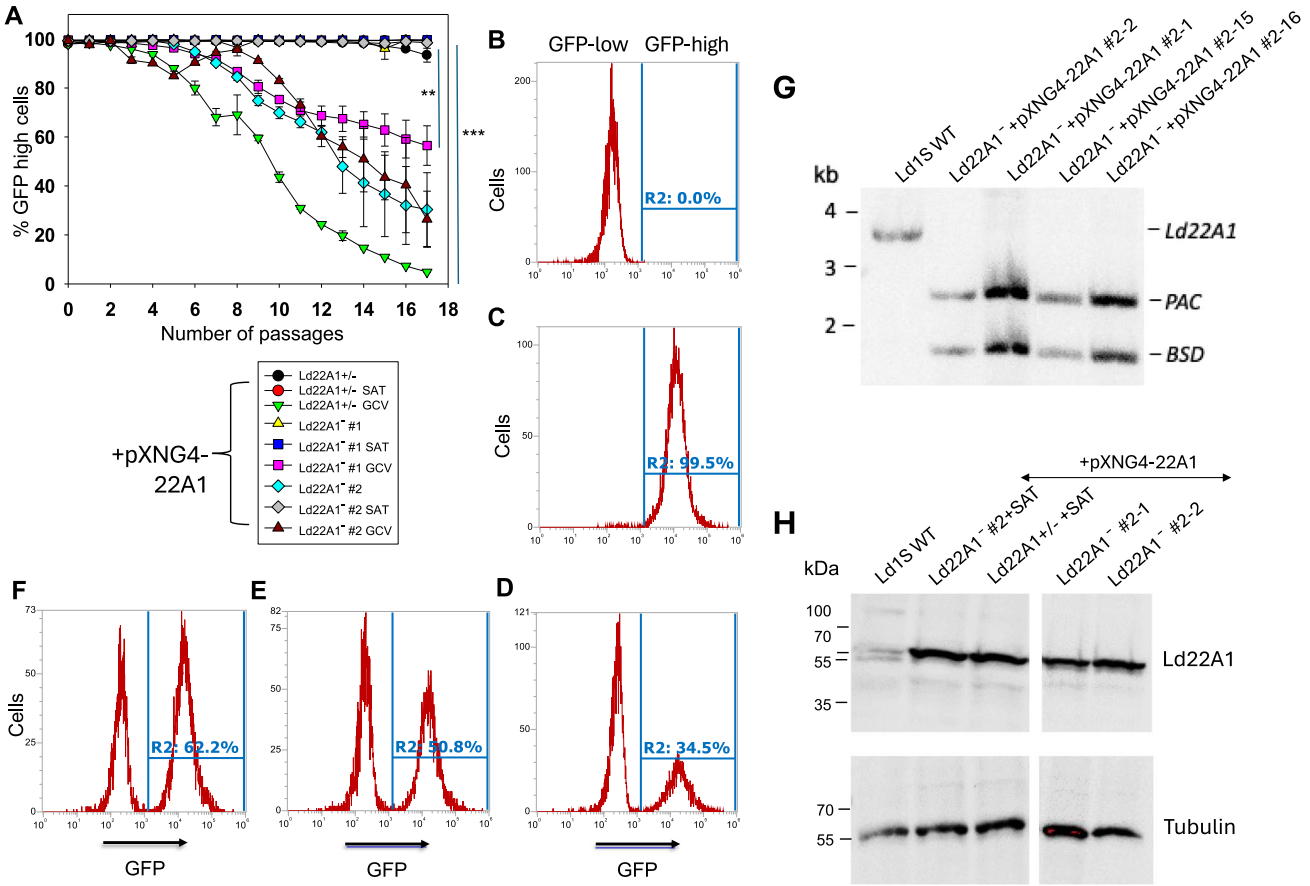

Fig. 4 | CYP5122A1 is indispensable during the promastigote stage. **A** Promastigotes were continuously cultivated in the presence or absence of ganciclovir (GCV) or nourseothricin (SAT) and passed every three days. Percentages of GFP-high cells were determined for every passage. Symbols and error bars represent the means and standard deviations from three independent repeats. Two-tailed ANOVA without adjustment (**$p < 0.01$, ***$p < 0.001$). Source data are provided as a Source Data file. After 14 passages, WT (**B**) and Ld22A1⁻+pXNG4-22A1 #2 parasites grown in the presence of SAT (**C**) or GCV (**D**) were analyzed by flow cytometry to determine the percentages of GFP-high cells (indicated by R2 in the histograms). Two clones (**E**: #2-1; **F**: #2-2) were isolated from the GFP-low population in D by FACS followed by serial dilution and amplification in the presence of GCV and analyzed for GFP expression by flow cytometry. **G** To verify the presence of episomal *CYP5122A1* allele, single clones isolated from the GFP-low (#2-1 and #2-2) and GFP-high (#2-15 and #2-16) populations of Ld22A1⁻+pXNG4-22A1 #2 parasites (**D**) were expanded in the presence of GCV and examined by Southern blot using a flanking region probe upstream of the *CYP5122A1* ORF probe. Bands corresponding to endogenous *CYP5122A1*, episomal *CYP5122A1*, and antibiotic resistance markers PAC/BSD were indicated. **H** To examine the CYP5122A1 protein levels, whole cell lysates from log phase promastigotes before (Ld22A1⁻ + pXNG4-22A1 #2 and Ld22A1 + /- +pXNG4-22A1) and after (#2-1 and #2-2) sorting were analyzed by Western blot using anti-LdCYP5122A1 (top) or anti-α-tubulin antibodies.

Ld22A1⁻ + pXNG4-22A1 grown in the presence of SAT (Fig. 4H). Together, these results supported that *CYP5122A1* is essential for *L. donovani* in the promastigote stage.

CYP5122A1 was essential for *L. donovani* amastigotes in mice

To investigate whether *CYP5122A1* is required during the amastigote stage, we infected the BALB/c mice with day 3 stationary phase promastigotes and treated them with either PBS (solvent control) or GCV. The weights of spleens from uninfected and infected mice were measured at 4- or 7-weeks post infection as a readout for splenomegaly, a symptom of VL (Fig. 5A). Parasite loads in infected spleens were determined by qPCR and limiting dilution analyses (Fig. 5B, C). As expected, the infection with Ld1S WT increased spleen weight in mice and the parasite growth was not affected by GCV treatment at weeks 4 and 7 post infection (Fig. 5A). Compared with the WT-infected group, the parasite loads in mice infected by Ld22A1 + /– were significantly lower (Fig. 5B, C), indicative of attenuated virulence. This could be partially reversed by the episomal expression of *CYP5122A1*, as we detected in mice infected by Ld22A1 + /– +pXNG4-22A1 or Ld22A1⁻ + pXNG4-22A1 with PBS treatment at week 4 post infection (Fig. 5B, C). For Ld22A1⁻+pXNG4-22A1, GCV treatment significantly reduced parasite loads at week 4 post infection, but the effect was less pronounced at week 7 post infection (Fig. 5B, C). It is possible that the effect of GCV (administered during the first two weeks) had worn down by week 7, allowing those persistent parasites to proliferate. Importantly, amastigotes of Ld22A1⁻ + pXNG4-22A1 from either PBS- or GCV-treated mice maintained much higher levels of the plasmid (average of 8-28 copies per cell) than Ld22A1 + /– +pXNG4-22A1 (average of <0.5 copies per cell in week 4 and <3 copies in week 7) (Fig. 5D). Together, these results demonstrated that *CYP5122A1* is indispensable for *L. donovani* amastigotes in mice.

Genetic manipulation of *CYP5122A1* altered sterol composition and affected the expression of surface glycoconjugates and promastigote stress responses

The effects of genetic manipulation of *CYP5122A1* on sterol synthesis were analyzed by LC-MS/MS (Table 1). Several 4,14-methylated sterols (lanosterol, 4CH_2OH-LS, and 4,14-DMZ) were significantly accumulated in Ld22A1 + /– during log and stationary phases, while CYP5122A1 overexpression led to reduced levels of these sterols. In addition, neither FF-MAS nor T-MAS (formed by lanosterol C14-demethylation by CYP51) was detected in the Ld1S WT, Ld22A1 + /–, Ld22A1 + /–

https://doi.org/10.1038/s41467-024-53790-5

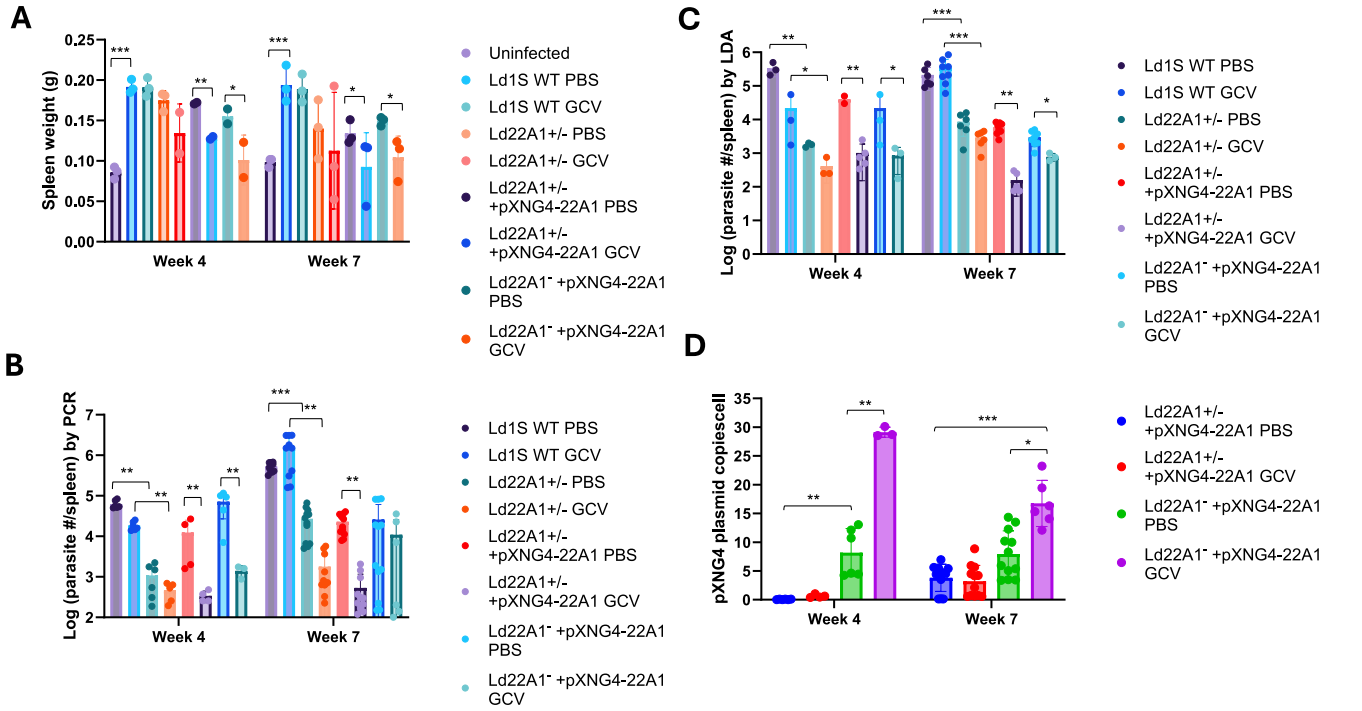

Fig. 5 | CYP5122A1 is indispensable during the amastigote stage. BALB/c mice were infected (i.p.) with day 3 stationary phase promastigotes (5 ×108 cells/mouse) and treated with GCV or PBS as described in *Methods*. **A** Spleen weights from uninfected and infected mice were measured at 4- or 7-weeks post infection. Parasite numbers in infected spleens were determined by qPCR (**B**) and limiting dilution assay (**C**) at the indicated times. **D** The pXNG4-22A1 plasmid copy numbers in amastigotes were determined by qPCR (#/cell ± SDs). Bars and error bars represent the means and standard deviations from 3 to 12 independent repeats. Two-tailed *t* test without adjustment (*$p < 0.05$, **$p < 0.01$, ***$p < 0.001$). Source data are provided as a Source Data file.

Table 1 | Effects of CYP5122A1 expression on the sterol profiles of *L. donovani* promastigotes at the log and stationary phases

	Sterols	Stationary phase			Log phase		
		Ld22A1+/− vs. Ld1S WT	Ld22A1+/− +pXNG4-22A1 vs. Ld1S WT	Ld22A1- +pXNG4-22A1 vs. Ld1S WT	Ld22A1+/− vs. Ld1S WT	Ld22A1+/− +pXNG4-22A1 vs. Ld1S WT	Ld22A1- +pXNG4-22A1 vs. Ld1S WT
4- and/or 14-methylated sterols	Lanosterol	9.3 ± 2.1	0.20 ± 0.03	0.38 ± 0.06	23 ± 5	0.35 ± 0.09	0.39 ± 0.16
	4-Hydroxylanosterol	3.3 ± 0.2	0.28 ± 0.07	0.23 ± 0.00	14 ± 1	0.21 ± 0.03	0.12 ± 0.04
	4,14-Dimethylzymosterol	2.0 ± 0.3	0.47 ± 0.06	0.24 ± 0.01	3.3 ± 0.8	0.20 ± 0.02	0.20 ± 0.07
	14-Methylzymosterol	0.81 ± 0.04	0.64 ± 0.05	0.74 ± 0.03	0.73 ± 0.01	0.52 ± 0.00	0.59 ± 0.20
	14-Methylfecosterol	ND	Accumulated	ND	ND	Accumulated	ND
	4-Methylzymosterol[a]	1.6 ± 0.1	2.3 ± 0.0	3.8 ± 0.1	1.1 ± 0.0	1.7 ± 0.2	1.0 ± 0.3
	FF-MAS	ND	ND	ND	ND	ND	ND
	T-MAS	ND	ND	ND	ND	ND	ND
4,14-demethylated sterols	Zymosterol[b]	1.2 ± 0.2	1.7 ± 0.1	0.89 ± 0.07	1.2 ± 0.0	1.6 ± 0.1	0.30 ± 0.11
	Fecosterol[a]	1.6 ± 0.1	2.3 ± 0.0	3.8 ± 0.1	1.1 ± 0.0	1.7 ± 0.2	1.0 ± 0.3
	Episterol[a]	1.6 ± 0.1	2.3 ± 0.0	3.8 ± 0.1	1.1 ± 0.0	1.7 ± 0.2	1.0 ± 0.3
	Cholesta-7,24-dienol[b]	1.2 ± 0.2	1.7 ± 0.1	0.89 ± 0.07	1.2 ± 0.0	1.6 ± 0.1	0.30 ± 0.11
5-dehydro sterols	7-Dehydrodesmosterol	0.75 ± 0.14	0.47 ± 0.07	0.14 ± 0.01	0.66 ± 0.10	0.48 ± 0.02	0.044 ± 0.019
	5-Dehydroepisterol	0.99 ± 0.18	0.83 ± 0.10	0.84 ± 0.07	0.82 ± 0.07	0.67 ± 0.03	0.30 ± 0.13
	Ergosta-5,7-dienol	1.2 ± 0.2	1.3 ± 0.2	2.0 ± 0.1	0.79 ± 0.08	0.78 ± 0.07	0.52 ± 0.23
	Ergostateraenol	1.0 ± 0.2	0.64 ± 0.10	1.0 ± 0.1	1.1 ± 0.1	0.96 ± 0.15	0.30 ± 0.10
	Ergosterol	1.0 ± 0.2	1.2 ± 0.1	1.8 ± 0.1	0.79 ± 0.14	1.0 ± 0.1	0.53 ± 0.16
	Cholesterol	1.2 ± 0.2	1.2 ± 0.0	1.5 ± 0.0	0.87 ± 0.07	0.89 ± 0.07	0.52 ± 0.17

The sterol levels in genetic mutants were normalized to the corresponding sterol levels in Ld1S WT. The values represent the mean ± 1/2 range ($n = 2$). Source data are provided as a Source Data file.
[a]Episterol, fecosterol and 4-methylzymosterol could not be chromatographically separated.
[b]Zymosterol and Cholesta-7,24-dienol could not be chromatographically separated.
ND not detected. Accumulated: This sterol was detected in the genetic mutants but not in Ld1S WT.

https://doi.org/10.1038/s41467-024-53790-5

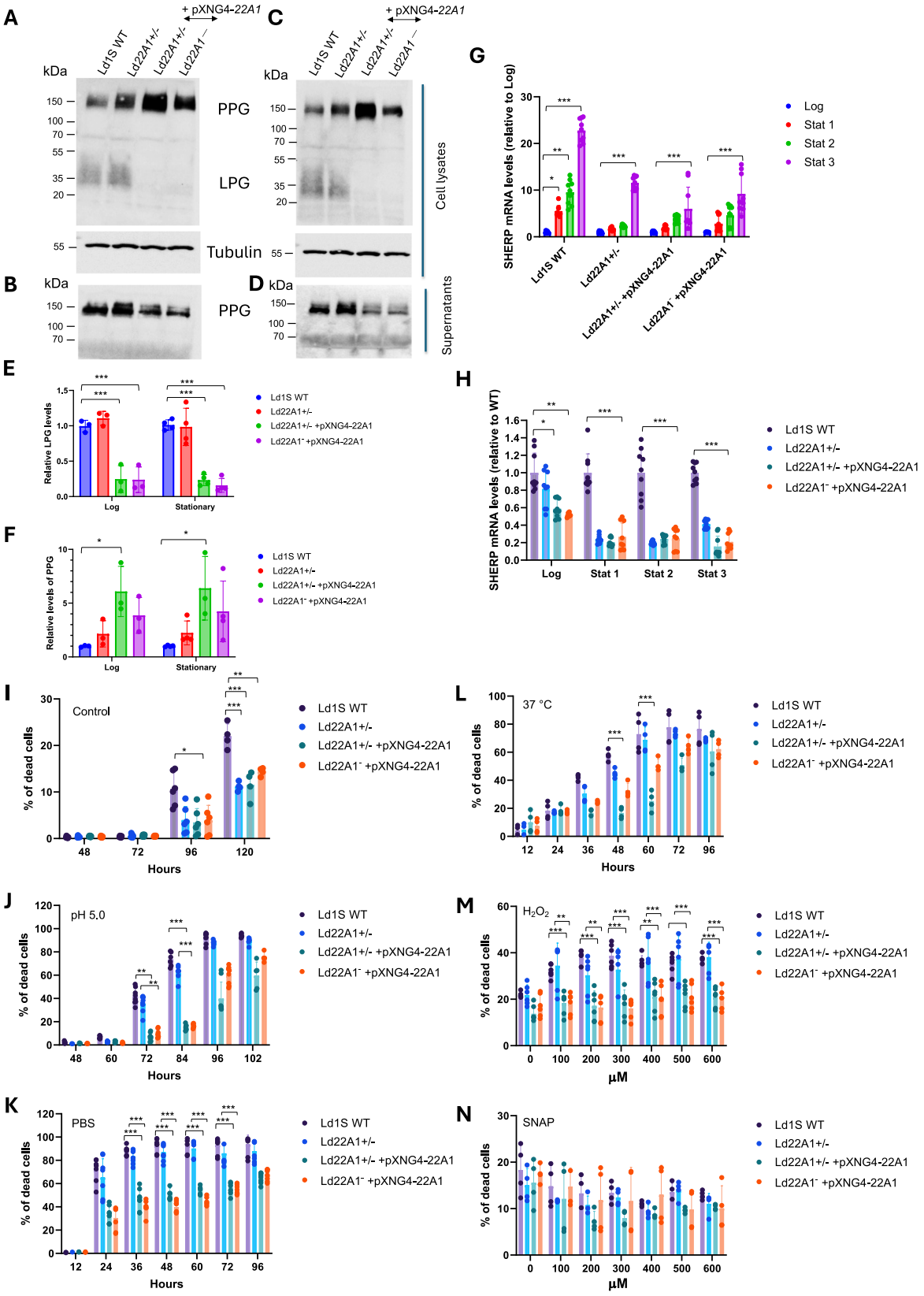

+pXNG4-22A1, or Ld22A1⁻ + pXNG4-22A1 promastigotes. This suggested that lanosterol C4-demethylation, rather than C14-demethylation, appears to be the dominant reaction during ergosterol biosynthesis in these parasites.

LPG and PPG are two major phosphoglycans in *Leishmania* promastigotes. They are critical for parasite attachment to the midgut of sand flies and for the establishment of infection in mammalian macrophages[38]. LPG is a glycosylphosphatidylinositol (GPI)-anchored cell surface molecule and has been identified as a virulence factor[39]. PPG has the GPI-anchored form present on the cell surface and the secreted form lacking in the GPI anchor[40]. Previously it was found that the levels of GPI-anchored molecules were affected by changes in sterol

Fig. 6 | Effects of CYP5122A1 half knockout and overexpression on promastigote differentiation. **A**–**F** CYP5122A1 overexpression alters the expression of LPG and PPG. Log phase (**A**, **B**) and stationary phase (**C**, **D**) promastigotes were subjected to Western blot analyses using the monoclonal antibody CA7AE (for LPG and PPG) or an anti-α-tubulin antibody (as loading control). A and **C**: whole cell lysates. **B** and **D**: culture supernatants. Relative expression levels of cellular LPG (**E**) and PPG (**F**) were determined with Ld1S WT as 1.0. **G**, **H** CYP5122A1 half knockout and overexpression reduces the expression of SHERP. Total RNA from log phase and stationary phase promastigotes were subjected to RT-qPCR analyses using primers for SHERP and 28S rDNA (as loading control). **G** Expression levels of SHERP in each parasite line from log phase to stationary phase using log phase levels as 1.0. **H** Expression levels of SHERP relative to Ld1S WT (as 1.0). **I**–**N** CYP5122A1 overexpression alters promastigote stress response. I–L Day 1 stationary phase promastigotes were incubated under various conditions and percentages of dead cells were determined by flow cytometry at the indicated times. **I** Complete M199 medium, 27 °C, pH7.4 (control). **J** Complete M199 medium, 27 °C, pH 5.0. **K** PBS, 27 °C, pH 7.4. **L** Complete M199 medium, 37 °C, pH 7.4. Day 1 stationary phase promastigotes were incubated in various concentrations of H_2O_2 (**M**) or SNAP (**N**) and percentages of dead cells were determined after 48 hours. Bars and error bars represent the means and standard deviations from three or four (**E** and **F**), three to nine (**G** and **H**), or three to six (**I** through **N**) independent repeats. Two-tailed *t* test without adjustment (*$p < 0.05$, **$p < 0.01$, ***$p < 0.001$). Source data are provided as a Source Data file.

Table 2 | In vitro antileishmanial activity and CYP inhibition of antifungal azoles and non-azole compounds

Compound	EC_{50} or IC_{50} (μM)			SI[c]
	EC_{50} (*L. donovani*)[a]	IC_{50} (LdCYP51)[b]	IC_{50} (LdCYP5122A1)[b]	
Imidazole				
Bifonazole	12 ± 1	0.057 ± 0.008	0.33 ± 0.07	5.7
Butoconazole	1.9 ± 0.4	0.073 ± 0.008	0.32 ± 0.07	4.4
Clotrimazole	5.0 ± 0.1	0.068 ± 0.004	0.26 ± 0.08	3.8
Econazole	9.4 ± 0.3	0.046 ± 0.004	0.47 ± 0.13	10
Fenticonazole	5.6 ± 0.3	0.081 ± 0.002	0.65 ± 0.08	8.0
Isoconazole	6.2 ± 0.5	0.049 ± 0.003	0.43 ± 0.04	8.8
Ketoconazole	22 ± 6	0.048 ± 0.007	0.42 ± 0.05	8.7
Miconazole	7.6 ± 0.7	0.057 ± 0.003	1.1 ± 0.2	19
Oxiconazole	3.9 ± 0.4	0.032 ± 0.002	0.62 ± 0.02	20
Sertaconazole	7.1 ± 0.5	0.064 ± 0.007	1.1 ± 0.2	17
Sulconazole	7.4 ± 0.6	0.064 ± 0.003	0.38 ± 0.06	5.9
Tioconazole	9.5 ± 0.6	0.054 ± 0.008	1.1 ± 0.2	20
Triazole				
Efinaconazole	15 ± 1	0.068 ± 0.002	6.2 ± 1.7	92
Fluconazole	>100[d]	0.96 ± 0.05	>100	>105
Isavuconazole	12 ± 0	0.043 ± 0.007	2.6 ± 0.7	60
Itraconazole	6.0 ± 1.1	0.049 ± 0.009	2.1 ± 0.4	43
Posaconazole	2.8[d]	0.059 ± 0.003	1.5 ± 0.3	25
Ravuconazole	12 ± 2	0.049 ± 0.008	12 ± 4	248
Terconazole	13 ± 1	0.083 ± 0.009	12 ± 3	140
Voriconazole	>100	0.085 ± 0.017	>100	>1176
Non azole compounds				
Miltefosine	2.7[e]	12 ± 1	43 ± 1	3.5
Pentamidine	14 ± 1	No inhibition at 100 μM	No inhibition at 100 μM	NA
Paromomycin	>50[e]	No inhibition at 100 μM	No inhibition at 100 μM	NA
Amphotericin B	0.14 ± 0.01	<25% inhibition at 10 μM	<25% inhibition at 10 μM	NA
DB766	0.036[f]	<30% inhibition at 30 μM	1.0 ± 0.1	<0.035

[a] Mean ± standard deviation ($n \geq 3$).
[b]Mean ± standard deviation ($n = 3$).
[c]SI (selectivity index) = IC_{50} against LdCYP5122A1/IC_{50} against LdCYP51.
[d]Published data from Feng et al. (ref. 18).
[e]IC_{50} vs. intracellular amastigotes from Wang et al. (ref. 45).
[f]IC_{50} vs. intracellular amastigotes from Wang et al. (ref. 45), see also Fig. 7.
Source data are provided as a Source Data file.

composition in *Leishmania*[11]. Considering the altered sterol profiles by genetic manipulation of CYP5122A1, we investigated if the expression of LPG and PPG was also impacted. Western blot analysis (Fig. 6A-F) showed that CYP5122A1 overexpression led to more cellular PPG but less secreted PPG in both log and stationary phases. In addition, the abundance of cellular LPG was significantly decreased in CYP5122A1 overexpressing cells, while the Ld22A1 + /– half knockout parasites were similar to Ld1S WT (Fig. 6E). Although it was unclear if these changes would have any implications on the parasite infectivity, the results provided more evidence of the association between the sterol composition and the synthesis of important virulence factors in *Leishmania*.

Alterations in LPG expression prompted us to investigate the impact of *CYP5122A1* genetic manipulation on promastigote differentiation as LPG modification is linked to the transition from replicative, non-infective procyclics to non-replicative, infective metacyclics[41,42]. As such, we examined the expression of a metacyclic stage-specific marker SHERP (small hydrophilic endoplasmic reticulum-associated protein)[43] (Fig. 6G, H). As expected, *SHERP* mRNA levels were relatively low in Ld1S WT and CYP5122A1 mutants during the log phase. Upon entering the stationary phase, their *SHERP* expression levels were significantly increased. However, the degree of SHERP induction in stationary phase was much less pronounced in comparison to WT (Fig. 6G). After normalizing the expression levels of *SHERP* in mutants to those in WT, we observed that *CYP5122A1* half knockout and overexpression significantly reduced the *SHERP* expression in both log and stationary phases (Fig. 6H).

We then assessed the ability of *CYP5122A1* mutants to withstand different types of stress in stationary phase when promastigotes differentiate from procyclics to metacyclics. Under the standard culture conditions (complete M199 medium, pH 7.4, 27 °C), less than 1% of dead cells were seen in stationary phase promastigotes after 72 h of incubation (Fig. 6I). Notably, *CYP5122A1* mutants displayed better survival in late stationary phase (96-120 h post inoculation). Acidic pH is one of the environmental stresses imposed on the *Leishmania* when they reside in the phagolysosome of macrophages. Here, when promastigotes were cultivated at pH 5.0 for 84 h, the percentage of dead cells was less than 20% in CYP5122A1 overexpressors but reached over 60% in Ld1S WT and Ld22A1 + /– (Fig. 6J). The increased tolerance of Ld22A1 + /– +pXNG4-22A1 and Ld22A1$^-$ + pXNG4-22A1 to stress was also evident in their responses to starvation. After incubation in PBS in the absence of nutrients for 36 h, they had ~40% of dead cells whereas almost 90% of the WT and Ld22A1 + /– cells did not survive (Fig. 6K). When the incubation temperature was set at 37 °C to mimic the mammalian body temperature, the percentage of dead cells increased slower in CYP5122A1 overexpressors than in Ld1S WT at 48-60 h post incubation (Fig. 6L). Apart from physical stresses, *Leishmania* parasites would encounter reactive oxygen and nitrogen species which are produced by macrophages as part of the host defense response[44]. To evaluate their resistance to oxidative or nitrosative stress[44], parasites were incubated in various concentrations of H_2O_2 or SNAP (Fig. 6M, N). CYP5122A1 overexpressors had superior viability than WT and Ld22A1 + /– at H_2O_2 concentrations up to 600 μM ($p < 0.001$) but exhibited no significant difference in response to SNAP. Taken together, CYP5122A1 overexpression rendered the cells more resistant to hostile environment.

Table 3 | Effects of different CYP inhibitor treatments on the sterol profile of LV82 promastigotes

Sterol Group	Sterol name	20 μM clotrimazole vs. DMSO	50 μM voriconazole vs. DMSO
4- and/or 14-methylated sterols	Lanosterol	2.7 ± 0.9**	1.6 ± 0.2
	4CH_2OH-LS	2.3 ± 0.5	0.83 ± 0.09
	4,14-Dimethylzymosterol	43 ± 18***	17 ± 2**
	14-Methylzymosterol	2.3 ± 0.4**	8.0 ± 1.0**
	14-Methylfecosterol	Accumulated[a],***	Accumulated[a],***
	4-Methylzymosterol[b]	0.025 ± 0.013***	0.18 ± 0.06**
	FF-MAS	Not detected	Not detected
	T-MAS	Not detected	Not detected
4,14-demethylated sterols	Zymosterol[c]	0.018 ± 0.006**	0.067 ± 0.034**
	Fecosterol[b]	0.025 ± 0.013***	0.18 ± 0.06**
	Episterol[b]	0.025 ± 0.013***	0.18 ± 0.06**
	Cholesta-7,24-dienol[c]	0.018 ± 0.006**	0.062 ± 0.030**
5-dehydro sterols	7-Dehydrodesmosterol	0[d],**	0[d],**
	5-Dehydroepisterol	0.20 ± 0.04**	0.078 ± 0.043***
	Ergosta-5,7-dienol	0.79 ± 0.26	0.39 ± 0.11**
	Ergostatetraenol	0 [d],**	0.086 ± 0.027**
	Ergosterol	0.26 ± 0.07**	0.30 ± 0.08***
Exogenous	Cholesterol	1.1 ± 0.2	0.88 ± 0.07

The sterol levels in inhibitor-treated parasites were normalized to the corresponding sterol levels in DMSO-treated parasites. The values represent mean ± standard deviation. Each ratio is an average of three individual experiments conducted on separate days. Each experiment had biological triplicates. Source data are provided as a Source Data file.

[a]This sterol was detected in inhibitor-treated samples but not in vehicle-treated samples

[b]Episterol, fecosterol and 4-methylzymosterol could not be chromatographically separated.

[c]Zymosterol and Cholesta-7,24-dienol could not be chromatographically separated.

[d]This sterol was detected in vehicle-treated samples but not in inhibitor-treated samples.

, * unpaired two-tailed *t*-test (**$P < 0.01$; ***$P < 0.001$).

Dual inhibition of CYP5122A1 and CYP51 was required for optimal antileishmanial activities by antifungal azoles

A panel of twenty marketed antifungal azole drugs was evaluated for their inhibitory activities against *L. donovani* CYP5122A1 and CYP51, along with several other classical antileishmanial agents (Table 2). Results of the inhibition assays showed that all tested antifungal azoles were potent inhibitors of CYP51 (IC_{50}s: 0.032 – 0.96 μM) but exhibited much weaker inhibition against CYP5122A1 (IC_{50}s ranging from 0.26 to over 100 μM). Specifically, voriconazole and fluconazole marginally inhibited CYP5122A1 at a concentration as high as 100 μM (< 28% and 20% inhibition, respectively). Voriconazole was the most selective inhibitor of CYP51 (> 1176-fold over CYP5122A1) and clotrimazole was the least selective one (3.8-fold). DB766, an antileishmanial arylimidamide[45], was identified as a selective inhibitor of CYP5122A1 (> 30-fold over CYP51). Two selective CYP51 inhibitors (voriconazole and fluconazole) and two dual CYP51/CYP5122A1 inhibitors (clotrimazole and posaconazole) were further assessed for their binding modes with the two CYP enzymes by UV-Vis spectrophotometric analysis (Supplementary Fig. 10). Clotrimazole exhibited type II binding to both CYP51 and CYP5122A1, indicating that the nitrogen in its imidazole group was directly coordinated with the heme iron at the active site. Posaconazole exhibited type II binding to CYP51, but a type II-like binding to CYP5122A1 (the trough peak at around 410 nm is absent). Fluconazole and voriconazole elicited type II binding with CYP51 but no specific responses with CYP5122A1, consistent with the observation that they were CYP51-selective inhibitors. Moreover, we evaluated the effect of azole antifungal drugs on the proliferation of *L. donovani* LV82 promastigotes (Table 2 and Supplementary Fig. 11). Of these 20 compounds tested, twelve displayed EC_{50} values < 10 μM, while another six azoles exhibited EC_{50} values between 10 μM and 25 μM. Interestingly, voriconazole and fluconazole, the weakest inhibitors of CYP5122A1, were the least effective at inhibiting parasite growth with EC_{50} values > 100 μM. A similar effect was also observed on intracellular *L. donovani* parasites in an infected peritoneal macrophage assay, where posaconazole was more effective than fluconazole (Supplementary Fig. 12). These results suggested that dual inhibitors of CYP51 and CYP5122A1 were more likely to inhibit *L. donovani* growth. Next, we examined leishmanicidal vs. leishmanistatic effect of dual inhibitors of CYP51 and CYP5122A1 and found that posaconazole and butaconazole both displayed a leishmanistatic effect, in contrast to the leishmanicidal effect of amphotericin B (Supplementary Fig. 13).

Sterol analysis of LV82 promastigotes showed that, as expected, both clotrimazole (dual CYP51 and CYP5122A1 inhibitor) and voriconazole (selective CYP51 inhibitor) treatments resulted in the depletion of 4,14-demethylated and 5-dehydro sterols in the downstream pathway of ergosterol biosynthesis, and the accumulation of some 4- and/or 14-methylated sterols (Table 3). However, the extent of change and identities of sterols impacted were different between the two treatments. Lanosterol and 4,14-DMZ, which are the substrates of CYP5122A1 and CYP51, were accumulated to a greater extent in the cells treated with clotrimazole than with voriconazole. Also, 14-methylzymosterol, an intermediate possessing the 14-methyl group but lacking methyl groups at C4, accumulated to an approximately 4-fold greater extent in parasites treated with voriconazole, a selective inhibitor of CYP51, compared to parasites treated with clotrimazole, a compound that inhibits both CYP51 and CYP5122A1. Indeed, the effects of clotrimazole and voriconazole on leishmanial sterol profiles were similar to those observed with posaconazole and fluconazole, respectively[18]. These results showed that in *L. donovani*, lanosterol undergoes C4-demethylation catalyzed by CYP5122A1 and inhibition of both CYP5122A1- and CYP51-mediated reactions by dual inhibitors like clotrimazole and posaconazole blocked ergosterol biosynthesis at earlier steps with a greater extent and produced better antileishmanial effects than the selective CYP51 inhibitors voriconazole and fluconazole.

https://doi.org/10.1038/s41467-024-53790-5

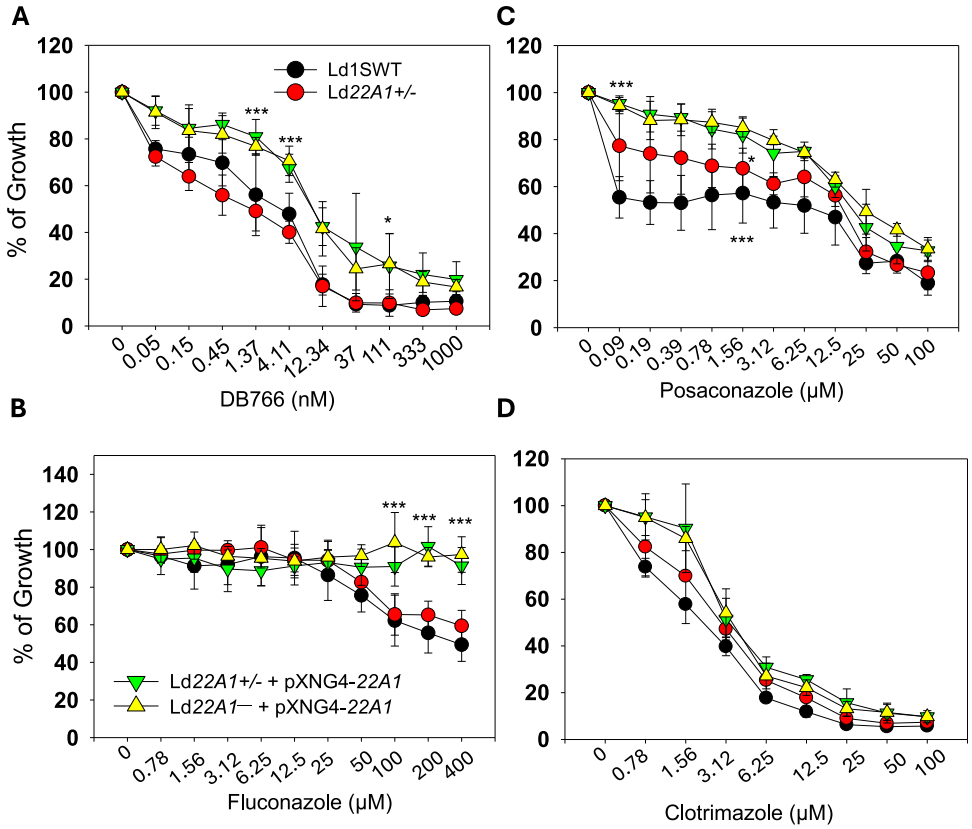

Fig. 7 | CYP5122A1 overexpression confers resistance to a subset of CYP5122A1 inhibitors. Log phase promastigotes were inoculated in various concentrations of DB766 (**A**), fluconazole (**B**), posaconazole (**C**) or clotrimazole (**D**); and culture densities were determined after 48 hours. Percentages of growth were indicated relative to control cells grown in the absence of inhibitors. Symbols and error bars represent the means and standard deviations from three independent repeats. Two-tailed ANOVA without adjustment (*$p < 0.05$, ***$p < 0.001$). Source data are provided as a Source Data file.

Sensitivity of CYP5122A1 half knockouts and overexpressors to CYP5122A1-selective and dual inhibitors

To test whether CYP5122A1 under- or over-expression affected the susceptibility to CYP5122A1-selective and dual inhibitors, we measured the growth of Ld1S WT and CYP5122A1 mutant promastigotes in the presence or absence of different inhibitors (Fig. 7). Compared to Ld1S WT and Ld22A1 + /–, CYP5122A1 overexpressors were more resistant to the CYP5122A1-selective inhibitor DB766 (Fig. 7A, EC_{50} = ~ 12 nM for overexpressors vs 1-4 nM for WT and Ld22A1 + /–), suggesting that an increased level of CYP5122A1 can bind and buffer the effect of this inhibitor. CYP5122A1 overexpressors also led to increased resistance to the CYP51 selective inhibitor fluconazole (Fig. 7B). For the dual inhibitor posaconazole, Ld1S WT showed a bi-phasic response with 0.1 μM being sufficient to reach EC_{50}, while more than 12 μM was needed to inhibit growth further (Fig. 7C). In contrast, CYP5122A1 overexpressors were more resistant to posaconazole (EC_{50} = ~25 μM), indicating that increased production of this enzyme can protect parasites against this dual inhibitor. An intermediate effect was observed with Ld22A1 + /–, which suggests compensatory changes in these half knockout parasites. Finally, no significant differences were detected between Ld1S WT and *CYP5122A1* mutants in sensitivity to clotrimazole, another dual inhibitor (Fig. 7D). Together, these studies suggest that increased production of CYP5122A1 confers heightened resistance to a subset of single and dual inhibitors.

Discussion

Sterol C4-demethylation is a vital step in ergosterol/cholesterol biosynthesis (Supplementary Fig. 1) and this step has been found to differ across biological kingdoms. In vertebrates, plants, and fungi, three enzymes function sequentially to remove the lanosterol C4-methyl groups: a nonheme iron-dependent sterol C4-methyl oxidase (SMO or Erg25), an NAD(P)-dependent 3β-hydroxysteroid dehydrogenase/C4-decarboxylase (3βHD/D or Erg26), and an NADPH-dependent 3-ketosteroid reductase (3-SR or Erg27)[19–21]. In some myxobacteria like *Methylococcus capsulatus*, sterol C4-demethylation is catalyzed by two enzymes that are phylogenetically and biochemically distinct from those in eukaryotes: SdmA (acting as SMO) and SdmB (may affect both decarboxylative oxidation and ketoreduction at C-3)[46]. Animals and yeast only have one sterol C4-methyl oxidase which is involved in the iterative removal of the two C4-methyl groups from sterols[19,47]. First, sterol C4-methyl oxidase converts the 4,4-dimethylated sterol substrate to a 4α-carboxylate metabolite, which subsequently decarboxylates to remove the first C4-methyl group. To maintain the stereochemical recognition by the enzyme during the removal of the second C4-methyl group, the remaining methyl group at the 4β-(axial) position epimerizes during the decarboxylation reaction to the 4α-(equatorial) position to form the 4-methyl 3-ketosteroid product. The 3-keto sterol is then reduced by 3-ketosteroid reductase to form the 3β-hydroxy sterol which has the last C4α-methyl group ready for another round of C4-demethylation[48]. To date, the sterol C4-demethylation process in *Leishmania* protozoa was largely unknown and often assumed to be similar to the one in fungi, which may be unwise as our recent work has shown that leishmanial ERG25 (orthologous to the yeast ERG25) was not required for sterol C4 demethylation in *L. major*[49].

In this study, we identified leishmanial CYP5122A1 as a sterol C4-methyl oxidase and unveiled a previously unrecognized important difference in the sterol C4-demethylation process between *Leishmania* and other species. Leishmanial CYP5122A1 was found to be responsible for oxidizing the lanosterol C4α-methyl group (C28-Me) into first a

hydroxyl, then an aldehyde, and finally a carboxylate/formyloxy metabolite, based on the NMR structural elucidation of the aldehyde metabolite (Fig. 3 and Supplementary Fig. 6). This is also further supported by other observations as follows. First, CYP5122A1 oxidized 4,14-DMZ, which has an α-configuration at both C4- and C14-methyl groups[18], and elicited a type-I binding with 4,14-DMZ (Fig. 1A). It also showed a type I binding specificity to C4-methylated sterols, whereas CYP51 preferred C14-methylated sterols (Fig. 1B). Second, CYP5122A1 converted 4,14-DMZ into a hydroxylated product (peak **15** in Fig. 2B) that is different from the C14-hydroxylmethyl product formed by CYP51 (peak **11** in Fig. 2B), indicating that CYP5122A1 likely acted on the C4-methyl group, rather than the C14-methyl group of 4,14-DMZ. Lastly, C4-methylated substrates (lanosterol, 4CH_2OH-LS, and 4,14-DMZ) were accumulated in *L. donovani* promastigotes when CYP5122A1 was either chemically inhibited (by clotrimazole; Tables 2 and 3) or genetically suppressed (Ld22A1 + /– heterozygotes; Supplementary Fig. 9 and Table 1).

This is the first report of a CYP-mediated sterol C4-methyl oxidation. Intriguingly, genes encoding CYP5122A1-like proteins were also identified in *T. brucei* and *T. cruzi* which are the causative agents of two important human parasitic diseases, African trypanosomiasis and Chagas disease, respectively. Their protein sequences are 50 – 53% identical to leishmanial CYP5122A1[27] and thus belong to the same CYP5122 family. Results from our study could shed light on the roles of these counterparts in *Trypanosoma*. It is unknown whether trypanosomal CYP5122A1 enzymes possess the same biochemical function or exhibit the same inhibition profile as the leishmanial CYP5122A1 enzyme. Moreover, enzymes that are involved in the C4-demethylation process after C4-oxidation in *Leishmania* (i.e., dehydrogenase/decarboxylase and reductase) remain uncharacterized, let alone other enzymes responsible for the multi-step conversion of lanosterol to ergosterol in these parasites. An ortholog of yeast Erg25 has been found in the *Leishmania* genome but its function remains to be characterized[50]. Tulloch et al.[29] recently characterized a leishmanial CYP reductase (P450R1) and suggested that this reductase may be a bona fide CYP reductase shuttling electrons from NADPH to CYP51. As such, the sterol biosynthetic pathway in protozoa warrants future dedicated investigation to fully understand the unique sterol biology of these single cell parasites. As demonstrated in this study, it is premature to assume these protozoan parasites behave like fungi or mammalian species.

The essentiality of *CYP5122A1* was first investigated in *L. donovani* promastigotes by using the homologous replacement approach[27]. Deleting both alleles of *CYP5122A1* was found to be lethal, which suggested that the gene is required for parasite survival. However, failure to obtain the null mutant in this way is often considered weak evidence for gene essentiality[51]. In the present study, the more rigorous forced plasmid shuffle approach was applied to examine the gene essentiality. We were able to generate the null mutant transfected with the plasmid containing *CYP5122A1* and a negative selection marker (TK). Null mutants without the episomal *CYP5122A1* could not survive. In the presence of negative selection, the parasites lacking in the plasmid would be favored, yet retention of the plasmid was observed in parasites after multiple passages. This provided compelling evidence supporting the essentiality of *CYP5122A1* in *L. donovani* promastigotes. Moreover, an equivalent assessment was conducted during the amastigote stage of the parasite life cycle. Unlike promastigotes, intracellular amastigotes live in a semi-quiescent state characterized by a slower replication rate, a reduced bio-energetic level, and a stringent metabolic response[52,53]. In particular, amastigotes acquire most of the sterols by salvage from the host although they retain the capacity of de novo synthesis[54]. It was observed that cholesterol was much more abundant than ergostane-based sterols in amastigotes[11]. In view of such different sterol profiles during the *Leishmania* life cycle, we investigated whether CYP5122A1 was still essential during the amastigote stage using a mouse model of visceral leishmaniasis infection. Under the pressure of negative selection, the null mutant with episomal complementation of *CYP5122A1* was able to proliferate in mice at a reduced capacity comparing to Ld1S WT and the plasmid was highly retained. These results demonstrate the essentiality of *CYP5122A1* in *L. donovani* amastigotes, as previously reported for other genes[55,56], which is critical for the genetic validation of CYP5122A1 as a drug target. It is of importance to determine whether the role of CYP5122A1 is conserved among other trypanosomatids in future studies. To fully exploit this target for antileishmanial drug discovery, determination of CYP5122A1 protein structure is also of importance to enable structure-based drug design, complementing high-throughput screening of CYP5122A1 inhibitors based on the BFC fluorescence inhibition assay developed in this study.

Antifungal azole drugs have been assessed for their potential to be used as antileishmanial agents. Studies showed that they were potent inhibitors of leishmanial CYP51 that can block ergosterol biosynthesis, but it was not fully understood why they had vastly different antileishmanial effects in vitro[14,15,57]. In this study, we screened a panel of twenty marketed antifungal azole drugs for the inhibition of CYP51 and CYP5122A1 using a fluorescence-based inhibition assay. Based on the selectivity towards the CYP enzymes, they were grouped into CYP51-selective inhibitors (e.g., fluconazole and voriconazole) and dual inhibitors of both CYP enzymes (e.g., posaconazole and clotrimazole). Overall, dual inhibitors exhibited higher antileishmanial activities against LV82 promastigotes than CYP51-selective inhibitors. This supports the critical role of CYP5122A1 in determining the azole activities against the parasites. When designing new compounds that target sterol biosynthesis in *Leishmania*, inhibiting both CYP51 and CYP5122A1 or inhibiting CYP5122A1 alone may be a better option than inhibiting CYP51 alone. A previous study on a potent antileishmanial arylimidamide DB766 implicated CYP5122A1 in its antileishmanial action[28], which was supported by our finding that DB766 is a strong CYP5122A1 inhibitor with IC_{50} of 1.0 ± 0.1 μM, although additional unknown mechanisms are likely involved to account for the potent antileishmanial activity of this compound with EC_{50} values ranging from 0.004 to 0.5 μM against multiple *Leishmania* species[45] (Fig. 7A). Future studies to identify alternative antileishmanial mechanisms of action of DB766 are hence warrantied to validate these targets and develop new hits that outperform DB766 in both activity and safety. In addition, future studies to identify CYP5122A1 inhibitors are also warranted to demonstrate if inhibiting CYP5122A1 is a viable pathway for antileishmanial drug development, such as our latest structure activity relationship study on N-substituted-4-(pyridin-4-ylalkyl)piperazine-1-carboxamides and related compounds as CYP51 and CYP5122A1 inhibitors[58].

When analyzing the sterol profiles of azole-treated promastigotes along with our previous findings[18], we found that CYP51-selective inhibitors and dual inhibitors resulted in distinct patterns of sterol accumulation. The underlying cause could be the branched ergosterol biosynthesis pathway that we previously proposed (Supplementary Fig. 1)[18]. Lanosterol, the substrate of both CYP51 and CYP5122A1, can undergo either a C4- or C14-demethylation reaction. Dual inhibitors caused lanosterol accumulation by inhibiting both reactions whereas CYP51-selective inhibitors would allow C4-demethylation to proceed. Furthermore, sterol analysis of genetic mutants showed accumulation of 4,14-methylated sterols (lanosterol, 4CH_2OH-LS, and 4,14-DMZ) in *Ld22A1* + /– and down-regulation in CYP5122A1 overexpressors (*Ld22A1* + /– +pXNG4-22A1 and *Ld22A1*$^-$+pXNG4-22A1), suggesting that C4-demethylation, rather than C14-demethylation, is the dominant reaction for lanosterol metabolism in *Leishmania*. This is further supported by the lack of detection of FF-MAS and T-MAS in the *Leishmania* parasites (Tables 1 and 3), which were expected to be formed by the lanosterol C14-demethylation catalyzed by CYP51.

There are several possible reasons for CYP5122A1 being essential to both *L. donovani* promastigotes and amastigotes. First, ergostane-based sterols are crucial and host-derived cholesterol is insufficient for maintaining the cell membrane rigidity. Second, the accumulation of 4,14-methylated sterols (e.g., lanosterol) and 4-methylated sterols have detrimental effects on *Leishmania* parasites. It has been found that the lipid domain/raft formation in the biological membranes is dependent on the sterol component having a structure that allows tight packing with lipids[59]. Ergosterol is conformationally and dynamically more restricted than cholesterol and has a higher tendency to promote lipid domain formation. Lanosterol is the bulkiest molecule among these three and is the least effective in inducing lipid packing[60,61]. Therefore, changes in sterol compositions could affect the lipid domains which have been implicated in numerous cellular processes. It was reported that the accumulation of C4-methyl sterols might serve as a signal for low oxygen and cell stress in fission yeast[62]. Similarly, C4-methyl sterols were also important for stress and hypoxia adaption in *Aspergillus fumigatus*[63]. However, whether C4-methyl sterol intermediates have any biological impacts on *Leishmania* parasites requires further investigation.

Notably, CYP5122A1 half knockout and overexpressors resulted in lower levels of *SHERP* expression relative to Ld1S WT in both log and stationary phases. SHERP, expressed predominantly in metacyclic parasites, is required for *Leishmania* metacyclogenesis in sand flies[64,65]. Studies suggested that it may function in modulating cellular processes related to membrane organization and/or acidification[66,67]. Reduction of SHERP expression suggests that endogenous CYP5122A1 plays a role in promastigote differentiation. In addition, CYP5122A1 overexpression led to delayed growth, different expression pattern for LPG/PPG, and altered stress responses (Fig. 6; and Supplemental Fig. 9A). Given that CYP5122A1 overexpression did not impact the bulk sterol composition but caused the depletion of 4-methylated sterols, it is likely that these low level intermediates serve as a signal to modulate promastigote differentiation. Finally, while dual inhibitors exhibited potent anti-proliferation effect, CYP5122A1 overexpression conferred significant protection (Fig. 7), which reinforced the importance of sterol C4-demethylation in *Leishmania*.

In summary, our study demonstrated that CYP5122A1 is a sterol C4-methyl oxidase involved in the sterol C4-demethylation process in *Leishmania*. The essentiality of CYP5122A1 was verified in both *L. donovani* promastigotes in culture and intracellular amastigotes in vivo. Overexpression of CYP5122A1 resulted in growth delay, differentiation defects, increased tolerance to environmental stresses, and altered expression of surface glycoconjugates. Antifungal azoles acting as dual inhibitors of CYP51 and CYP5122A1 had higher antileishmanial activity against *L. donovani* promastigotes than CYP51-selective inhibitors, suggesting a new strategy to develop therapeutic agents to target the sterol biosynthetic pathway in *Leishmania*.

Methods

All mouse infection procedures were performed as per approved protocol by the Animal Care and Use Committee at Texas Tech University (PHS Approved Animal Welfare Assurance No A3629-01) and all animals were housed in air-conditioned rooms (20–25 °C, 40–60% humidity) with a 12-hour light–dark cycle. Collection of peritoneal macrophages from female CD-1 mice for the intracellular *L. donovani* assay and collection of *Leishmania* parasites from hamster spleens to infect the macrophages were performed according to protocols approved by the Animal Care and Use Committee at The Ohio State University (Protocol #: 2007A0129 and 2009A0229, respectively) and all animals were housed in air-conditioned rooms (20–24.4 °C, 30–70% humidity) with a 12-hour light–dark cycle.

Chemicals and reagents

Lanosterol (>=93% pure) and reduced nicotinamide adenine dinucleotide phosphate (NADPH) were obtained from Sigma-Aldrich (St. Louis, MO). 5α-Cholesta-8,24-dien-3β-ol (zymosterol), 14-demethyl-14-dehydrolanosterol (FF-MAS), 4,4-dimethylcholesta-8,24-dien-3β-ol (T-MAS), and cholesterol-d7 were purchased from Avanti Polar Lipids Inc (Alabaster, AL). 4α,14α-Dimethylzymosterol (4,14-DMZ) was isolated from the sterol extract of *L. tarentolae*[18]. Dilaurylphosphatidylcholine (DLPC), dimyristoylphosphatidylcholine (DMPC), and dimyristoylphosphatidylglycerol (DMPG) were either gifts from Dr. Philip Gao at the Protein Production Group, University of Kansas or purchased from Tokyo Chemical Industry Co., LTD. (Portland, OR) and Avanti Polar Lipids Inc. Emulgen 911 was purchased from Desert Biologicals (Phoenix, AZ). Reagents used in *Leishmania* work were purchased from Thermo Fisher Scientific (Waltham, MA) or VWR (Radnor, PA) unless otherwise specified. Azole antifungals were purchased from various vendors (Supplementary Table 1).

Cloning, expression, and purification

The CYP5122A1 and CYP51 enzymes used in this study were the truncated forms of the full-length proteins (XP_003861867.1 and XP_003859085.1) without the transmembrane domains (the first 60 and 31 amino acids for CYP5122A1 and CYP51 as shown in Supplementary Fig. 2). A solubility tag MAKKTSSKGKL[68] and a His-tag were added to the N- and C-terminus, respectively, to facilitate protein purification. Their gene sequences were incorporated into the pCWori vector (a gift from Dr. Emily Scott; University of Michigan) and confirmed by Sanger sequencing prior to expression (primer sequences in Supplementary Table 4). NEB® 5-alpha F'*Iq* competent *E. coli* (New England Biolabs) transformed with the plasmids were grown at 37 °C. When OD_{600} reached 0.6, isopropyl β-D-1-thiogalactopyranoside (IPTG; 0.7 mM; Gold Biotechnology) and δ-aminolevulinic acid (1 mM; Acros Organics) were added and then the *E. coli* culture was incubated at 25 °C and 200 rpm for 48 h. The cells were harvested by centrifugation at 6675 g for 30 min. Protein purification was performed as described previously[69]. The molecular weight and purity of the proteins were confirmed by SDS-PAGE.

The sequence encoding the C-terminal His-tagged *Trypanosoma brucei* NADPH-cytochrome P450 reductase (TbCPR; XP_828912.1) was incorporated into the pCWori vector and confirmed by Sanger sequencing (primer sequences in Supplementary Table 4). The protein expression procedure was similar to the one for CYP enzymes and the only difference was that IPTG (0.7 mM) and riboflavin (4 μg/mL) were added when OD_{600} was 0.6. The purification procedure was also modified from the one for CYP enzymes. TbCPR was purified by Ni-NTA chromatography followed by dialysis for 24 h in the buffer containing 50 mM Tris (pH 7.6), 10% glycerol, 0.1 mM EDTA, and 1 mM DTT. The molecular weight and purity of TbCPR were confirmed by SDS-PAGE.

Western blot analysis

Polyclonal antisera of CYP5122A1 and CYP51 were raised against the purified recombinant proteins in rats (gift from Dr. Jianming Qiu of the University of Kansas Medical Center). To determine the levels of CYP5122A1, CYP51, lipophosphoglycan (LPG), and proteophosphoglycan (PPG), promastigote lysates were boiled in SDS-containing sample buffer at 95-100 °C for 5 min and resolved by SDS-PAGE. After transfer to a PVDF membrane, blots were probed with rat anti-CYP5122A1 (1:500), rat anti-CYP51 (1:500), or monoclonal antibody CA7AE (1:1000, for LPG and PPG)[70] followed by HRP-conjugated anti-rat or anti-mouse secondary antibodies. Antibody to alpha-tubulin (Thermo Fisher Scientific) was used as the loading control. Similar experiments were performed to determine the LPG and PPG levels in the culture supernatant of stationary phase promastigotes.

UV-Vis spectroscopy

The ferric absolute spectra, carbon monoxide (CO) difference spectra, and substrate binding difference spectra for CYP51 and CYP5122A1 were recorded on a Cary 3500 UV/Vis spectrophotometer (Agilent) by following published protocols[32]. The active P450 content and the binding constant of sterol substrates were determined as described by Hargrove et al.[24].

Reconstitution of CYP51 and CYP5122A1 catalytic activity

The standard reconstitution reaction (100 µL) contained 1 µM CYP enzyme, 5 µM TbCPR, 50 µM substrate, and 50 µg/mL phospholipids (DLPC:DMPC:DMPG = 5:4:1, w/w/w) in 100 mM phosphate buffer (pH 6.2) with 3.3 mM $MgCl_2$. The reaction was initiated with the addition of 1 mM NADPH and then incubated at 37 °C for up to 1 h. To obtain the metabolites of lanosterol in the CYP5122A1-catalyzed reaction for NMR analysis, the reaction mixture was slightly modified, which contained the 2 µM CYP enzyme, 6 µM TbCPR, 20 µM lanosterol, and 50 µg/mL phospholipids in the same buffer (10 mL each reaction and a total of 770 mL). After adding 1 mM NADPH, the reaction was incubated at 37 °C for 2 h. The sterols in the reconstitution reactions were extracted and analyzed by liquid chromatography-tandem mass spectrometry (LC-MS/MS) as previously described[18].

Sterol purification

The crude sterol sample was dried under a vacuum using a rotary evaporator and redissolved in 1:1 (v/v) DMSO: tetrahydrofuran. Sterol purification was performed using an Agilent 1260 Infinity II HPLC system with a G7157A Agilent prep autosampler, a G7161A Agilent binary pump, a G7115A Agilent diode array detector, and a G1364E Agilent fraction collector. The sterols were separated on a Waters XBridge BEH C18 OBD prep column (19 mm × 250 mm, 5 µm). LC mobile phases consisted of (A) water containing 0.05% (v/v) difluoroacetic acid and (B) acetonitrile containing 0.05% (v/v) difluoroacetic acid. A gradient elution was used for purification, which began from 75% to 100% B over 10 min and held at 100% B for 35 min with a flow rate of 20 mL/ min. The detection wavelength was set at 214 nm and 254 nm.

NMR analysis

All NMR spectra were acquired on an Avance AVIII 500 MHz spectrometer equipped with a multinuclear BBFO cryoprobe. Approximately 2.1 mg of the purified sterol metabolite was dissolved in 0.5 mL of deuterated chloroform ($CDCl_3$). NMR experiments including ^1H, ^{13}C, HSQC, NOESY, and HMBC were recorded with extended runtimes. Chemical shifts are reported in ppm, and coupling constants are reported in Hz. The chemical shifts at 7.26 ppm and 77.15 ppm for proton and carbon spectra respectively are from residual $CHCl_3$ in $CDCl_3$ and were used as internal references. ^1H and ^{13}C NMR assignments of lanosterol were used as a reference for the structural assignment of the proposed sterol metabolite.

CYP inhibition assay

The inhibition assays for CYP5122A1 and CYP51 were carried out as described previously for leishmanial CYP51[69]. All tested compounds were dissolved in DMSO except miltefosine, pentamidine isethionate, paromomycin sulfate, and amphotericin B deoxycholate which were dissolved in water. Briefly, a CYP enzyme (50 nM) was incubated with the fluorogenic substrate 7-benzyloxy-4-trifluoromethylcoumarin (BFC; 50 µM) and various concentrations of test compounds in 100 mM phosphate buffer (pH 7.4) and 3.3 mM $MgCl_2$. Compound solvents (DMSO and water) were used as the negative control. The reaction was initiated with the addition of cumene hydroperoxide (100 µM), incubated at 37 °C, and monitored at an emission wavelength of 538 nm and an excitation wavelength of 410 nm on a Tecan Infinite® M200 Pro microplate reader. For test compounds, the percentage of inhibition at each concentration was calculated as $(1-RFU_{compound}/RFU_{control}) \times 100$, where RFU is the relative fluorescence unit. A plot of the percentage of inhibition versus the logarithm of the compound concentration was fit with the following two-parameter logistic equation to obtain the IC_{50} value (GraphPad Prism version 8.4.0):

$$y = \frac{100}{1 + (\frac{x}{IC_{50}})^{\text{Hill Slope}}} \quad (1)$$

Leishmania donovani 1S2D culture and genetic manipulations of *CYP5122A1*

Leishmania donovani strain 1S2D (MHOM/SD/62/1S-CL2D) clone LdBob promastigotes were cultivated at 27 °C in a complete M199 medium (M199 with 10% heat-inactivated fetal bovine serum and other supplements, pH 7.4)[71]. To monitor growth, culture densities were measured daily using a Beckman Z2 Cell Counter. Log phase promastigotes refer to replicative parasites at densities $<1.0 \times 10^7$ cells/ml, and stationary phase promastigotes refer to non-replicative parasites at densities $>2.0 \times 10^7$ cells/ml.

To delete chromosomal *CYP5122A1* alleles, the upstream and downstream flanking sequences of *CYP5122A1* (~1 Kb each) were amplified by PCR and cloned in the pUC18 vector (primer sequences in Supplementary Table 4). Genes conferring resistance to blasticidin (BSD) and puromycin (PAC) were cloned between the upstream and downstream flanking sequences to generate pUC18-KO-CYP5122A1:BSD and pUC18-KO- CYP5122A1:PAC, respectively. To generate the CYP5122A1 + /− heterozygotes (ΔCYP5122A1::BSD/CYP5122A1), wild-type (WT) *L. donovani* promastigotes were transfected with linearized BSD knockout fragment (derived from pUC18-KO-CYP5122A1:BSD) by electroporation and transfectants showing resistance to blasticidin were selected and later confirmed to be CYP5122A1 + /− by Southern blot as previously described[56]. To delete the second chromosomal allele of *CYP5122A1*, we used an episome-assisted approach as previously described for other genes[72]. First, the *CYP5122A1* open reading frame (ORF) was cloned into the pXNG4 vector to generate pXNG4-22A1 and introduced into CYP5122A1 + /− parasites. The resulting CYP5122A1 + /- +pXNG4-22A1 cell lines were then transfected with linearized PAC knockout fragment (derived from pUC18-KO-CYP5122A1:PAC) and selected with 15 µg/ml of blasticidin, 15 µg/ml of puromycin and 150 µg/ml of nourseothricin. The resulting *CYP5122A1* chromosomal null mutants with pXNG4-22A1 (ΔCYP5122A1::BSD/ΔCYP5122A1::PAC + pXNG4-CYP5122A1 or CYP5122A1$^-$ + pXNG4-22A1) were validated by Southern blot as previously described for other genes[56]. *Leishmania donovani* strain 1S2D *CYP5122A1* mutants are available for research and non-commercial use upon written request to the corresponding author with reasonable payment to cover costs of distribution.

Determination of in vitro antileishmanial activities of antifungal azole compounds in *CYP5122A1* mutants of *L. donovani* strain 1S2D

Stock solutions for test compounds were prepared at 10 mM in DMSO. To measure the antileishmanial activity of these inhibitors, log phase promastigotes were inoculated in complete M199 media at 2.0×10^5 cells/ml in 24-well plates (1 ml/well). Inhibitors were added to various concentrations and control wells contained DMSO only (0.1-0.5%). Culture densities were determined after 48 h using a Beckman Z2 Cell Counter.

Promastigote essentiality assay

L. donovani CYP5122A1 + /- +pXNG4-22A1, and CYP5122A1$^-$ + pXNG4-22A1 promastigotes were inoculated in complete M199 media at 1.0×10^5 cells/ml in the presence or absence of 50 µg/ml of GCV (the

negative selection agent) or 150 μg/ml of nourseothricin (the positive selection agent). Every three days, cells were reinoculated into fresh media with the same negative or positive selection agents, and percentages of GFP-high cells for each passage were determined by flow cytometry using an Attune NxT Acoustic Flow Cytometer. After 14 passages, individual GFP-high and GFP-low clones of CYP5122A1^{-}+pXNG4-22A1 were isolated by fluorescence-activated cell sorting (FACS), followed by serial dilution in 96-well plates and expanded in the presence of GCV and absence of nourseothricin. The GFP levels of selected clones were determined by flow cytometry.

Mouse infection

Female BALB/c mice (7-8 weeks old) were purchased from Charles River Laboratories International (Wilmington, MA). To determine whether CYP5122A1 is required during the intracellular amastigote stage, day 3 stationary phase promastigotes were injected into the peritoneal cavity of BALB/c mice (5.0×10^8 cells/mouse, 10 mice per group). For each group, starting from day one post infection, one-half of the mice received GCV at 7.5 mg/kg/day for 14 consecutive days (0.5 ml each, intraperitoneal injection), while the other half (control group) received an equivalent volume of sterile PBS. At 4- or 7-weeks post infection, mice were euthanized through a controlled flow of CO_2 asphyxiation and infected spleens were isolated and homogenized. Parasite numbers in spleen homogenates were determined by limiting dilution assay[73] or qPCR as described below.

Quantitative PCR (qPCR)

To determine parasite loads in infected mice, genomic DNA was extracted from spleen homogenate and qPCR reactions were run in triplicates using primers targeting the 28S rRNA gene of *L. donovani*[56]. Cycle threshold (Ct) values were determined from melt curve analysis. A standard curve of Ct values was generated using serially diluted genomic DNA samples from *L. donovani* promastigotes (from 0.1 cell/reaction to 10^5 cells/reaction) and Ct values > 30 were considered negative. Parasite numbers in spleen samples were calculated based on their Ct values using the standard curve. Control reactions included sterile water and DNA extracted from the uninfected mouse spleen.

To determine pXNG4-22A1 plasmid levels in promastigotes and amastigotes, a similar standard curve was generated using serially diluting pXNG4-22A1 plasmid DNA (from 0.1 copy/reaction to 10^5 copies/reaction) and primers targeting the *GFP* region. qPCR was performed with the same set of primers on DNA samples from promastigotes or spleen and the average plasmid copy number per cell was determined by dividing the total plasmid copy number by the total parasite number based on Ct values.

To determine the transcript levels of SHERP (small hydrophilic endoplasmic reticulum-associated protein), total RNA was extracted from promastigotes and converted into cDNA using a high-capacity reverse transcription kit (Bio-Rad), followed by qPCR using primers targeting SHERP or 28S rRNA genes. The relative expression level of SHERP was normalized to that of 28 s rRNA using the $2^{-\Delta\Delta(Ct)}$ method[74]. Control reactions were carried out without leishmanial RNA and without reverse transcriptase.

Leishmania donovani 1S2D stress response assays

L. donovani promastigotes were cultivated in complete M199 media (pH 7.4) at 27 °C until they reach the stationary phase. For heat tolerance, promastigotes were incubated at 37 °C. To test their sensitivity to acidic pH, promastigotes were transferred to a pH 5.0 medium (same as the complete M199 medium except that the pH was adjusted to 5.0 using hydrochloric acid). For starvation response, promastigotes were transferred to PBS (pH 7.4). For resistance to oxidative or nitrosative stress, parasites were incubated in various concentrations of H_2O_2 or S-nitroso-N-acetylpenicillamine (SNAP). Cell viability was determined at the indicated times by flow cytometry after staining with 5 μg/ml of propidium iodide. Parasite growth was monitored using a Beckman Z2 Cell Counter.

Growth inhibition and sterol analysis experiments with *L. donovani* LV82 parasites

L. donovani LV82 (MHOM/ET/67/LV82) promastigotes were assayed to examine the effects of azole drugs on parasite growth and sterol composition according to methods detailed by Feng et al.[18]. In brief, low-pass LV82 promastigotes obtained by transforming amastigotes from infected hamster spleens were cultured in Schneider's *Drosophila* medium (Gibco) containing 25% heat-inactivated fetal bovine serum (Sigma-Aldrich) and penicillin-streptomycin (Gibco). Growth assays were performed after three-day incubation of promastigotes at 26 °C with or without azole drugs in the above medium containing 50 U/mL penicillin and 50 μg/mL streptomycin using 3-(4,5-dimethylthiazol-2-yl)−5-(3-carboxymethoxyphenyl)−2-(4-sulfophenyl)−2H-tetrazolium, inner salt (MTS):phenazine methosulfate (PMS) as an indicator of parasite growth as described earlier[18]. Absorbance values for individual wells measured at 490 nm were normalized to positive and negative controls, then normalized absorbance values were plotted against concentration using the R (drc) package[75] to acquire EC_{50} values and standard errors obtained by least square fitting. At least three independent experiments were used to determine the effect of different azole concentrations on parasite growth, with validity criteria for individual experiments outlined in Feng et al.[18]. Intracellular *L. donovani* assays with posaconazole and fluconazole were conducted as described by Joice et al.[76]. Samples for sterol analysis were obtained after incubating LV82 promastigotes treated for 24 hr at 26 °C with either vehicle (0.4% DMSO v/v), clotrimazole (20 μM), or voriconazole (50 μM). Promastigotes exposed to clotrimazole were maintained in Schneider's *Drosophila* medium containing 25% heat-inactivated FBS containing 100 U/mL penicillin and 100 μg/mL streptomycin and promastigotes exposed to voriconazole were cultured in Schneider's *Drosophila* medium containing 25% heat-inactivated FBS containing 50 U/mL penicillin and 50 μg/mL streptomycin. After exposure to azole drugs or vehicle, parasites were centrifuged, washed with PBS, and stored at −80 °C prior to analysis as mentioned earlier[18].

Statistical analysis

Unless otherwise specified, experiments were repeated three to six times. Symbols or bars represent mean values and error bars represent standard deviations. Differences between groups were assessed by one-way ANOVA (for three or more groups) or student *t* test (for two groups). Graphs were generated using Sigmaplot 13.0 (Systat Software Inc, San Jose, CA), or GraphPad Prism 10.0 (GraphPad Software, Boston, MA), or KaleidaGraph 4.5 (Synergy Software, Reading, PA), or R 4.1 (R Foundation for Statistical Computing, Vienna, Austria). *P* values were grouped as $p < 0.001$ (***), $p < 0.01$ (**), and $p < 0.05$ (*).

Reporting summary

Further information on research design is available in the Nature Portfolio Reporting Summary linked to this article.

Data availability

All data generated or analyzed during this study are included in this published article and its supplementary information files. Source data are provided with this paper.

References

1. Bates, P. A. Revising Leishmania's life cycle. *Nat. Microbiol* **3**, 529–530 (2018).
2. Kima, P. E. The amastigote forms of Leishmania are experts at exploiting host cell processes to establish infection and persist. *Int J. Parasitol.* **37**, 1087–1096 (2007).

3. Serafim, T. D. et al. Sequential blood meals promote Leishmania replication and reverse metacyclogenesis augmenting vector infectivity. *Nat. Microbiol* **3**, 548–555 (2018).
4. World Health Organization (WHO) Leishmaniasis - Key Facts [cited 2024 October 29th]. Available from: https://www.who.int/news-room/fact-sheets/detail/leishmaniasis.
5. Chappuis, F. et al. Visceral leishmaniasis: what are the needs for diagnosis, treatment and control? *Nat. Rev. Microbiol* **5**, 873–882 (2007).
6. Karmakar, S. et al. Preclinical validation of a live attenuated dermotropic Leishmania vaccine against vector transmitted fatal visceral leishmaniasis. *Commun. Biol.* **4**, 929 (2021).
7. Alves, F. et al. Recent development of visceral leishmaniasis treatments: successes, pitfalls, and perspectives. *Clin. Microbiol Rev.* **31**, e00048–18 (2018).
8. Sundar, S. & Singh, B. Emerging therapeutic targets for treatment of leishmaniasis. *Expert Opin. Ther. Targets* **22**, 467–486 (2018).
9. de Souza, W. & Rodrigues, J. C. Sterol biosynthesis pathway as target for anti-trypanosomatid drugs. *Interdiscip. Perspect. Infect. Dis.* **2009**, 642502 (2009).
10. Yao, C. et al. Attenuation of Leishmania infantum chagasi metacyclic promastigotes by sterol depletion. *Infect. Immun.* **81**, 2507–2517 (2013).
11. Xu, W., Hsu, F. F., Baykal, E., Huang, J. & Zhang, K. Sterol biosynthesis is required for heat resistance but not extracellular survival in leishmania. *PLoS Pathog.* **10**, e1004427 (2014).
12. Mukherjee, S., Moitra, S., Xu, W., Hernandez, V. & Zhang, K. Sterol 14-alpha-demethylase is vital for mitochondrial functions and stress tolerance in Leishmania major. *PLoS Pathog.* **16**, e1008810 (2020).
13. McCall, L. I. et al. Targeting Ergosterol biosynthesis in Leishmania donovani: essentiality of sterol 14 alpha-demethylase. *PLoS Negl. Trop. Dis.* **9**, e0003588 (2015).
14. Beach, D. H., Goad, L. J. & Holz, G. G. Jr. Effects of antimycotic azoles on growth and sterol biosynthesis of Leishmania promastigotes. *Mol. Biochem Parasitol.* **31**, 149–162 (1988).
15. Yamamoto, E. S. et al. Activity of fenticonazole, tioconazole and nystatin on New World Leishmania species. *Curr. Top. Med Chem.* **18**, 2338–2346 (2018).
16. Buckner, F. S. & Wilson, A. J. Colorimetric assay for screening compounds against Leishmania amastigotes grown in macrophages. *Am. J. Trop. Med Hyg.* **72**, 600–605 (2005).
17. de Macedo-Silva, S. T., Urbina, J. A., de Souza, W. & Rodrigues, J. C. In vitro activity of the antifungal azoles itraconazole and posaconazole against Leishmania amazonensis. *PloS one* **8**, e83247 (2013).
18. Feng, M. et al. Sterol profiling of Leishmania parasites using a new HPLC-tandem mass spectrometry-based method and antifungal azoles as chemical probes reveals a key intermediate sterol that supports a branched ergosterol biosynthetic pathway. *Int J. Parasitol. Drugs Drug Resist* **20**, 27–42 (2022).
19. Bard, M. et al. Cloning and characterization of ERG25, the Saccharomyces cerevisiae gene encoding C-4 sterol methyl oxidase. *Proc. Natl Acad. Sci. USA* **93**, 186–190 (1996).
20. Gachotte, D., Barbuch, R., Gaylor, J., Nickel, E. & Bard, M. Characterization of the Saccharomyces cerevisiae ERG26 gene encoding the C-3 sterol dehydrogenase (C-4 decarboxylase) involved in sterol biosynthesis. *Proc. Natl Acad. Sci. USA* **95**, 13794–13799 (1998).
21. Gachotte, D. et al. Characterization of the Saccharomyces cerevisiae ERG27 gene encoding the 3-keto reductase involved in C-4 sterol demethylation. *Proc. Natl Acad. Sci. USA* **96**, 12655–12660 (1999).
22. Rahier, A. Dissecting the sterol C-4 demethylation process in higher plants. From structures and genes to catalytic mechanism. *Steroids* **76**, 340–352 (2011).
23. Lepesheva, G. I. & Waterman, M. R. Sterol 14alpha-demethylase (CYP51) as a therapeutic target for human trypanosomiasis and leishmaniasis. *Curr. Top. Med Chem.* **11**, 2060–2071 (2011).
24. Hargrove, T. Y. et al. Substrate preferences and catalytic parameters determined by structural characteristics of sterol 14alpha-demethylase (CYP51) from Leishmania infantum. *J. Biol. Chem.* **286**, 26838–26848 (2011).
25. Friggeri, L. et al. Sterol 14alpha-demethylase structure-based optimization of drug candidates for human infections with the protozoan Trypanosomatidae. *J. Med Chem.* **61**, 10910–10921 (2018).
26. da Silva Santos-Junior, P. F., Schmitt, M., de Araujo-Junior, J. X. & da Silva-Junior, E. F. Sterol 14alpha-demethylase from Trypanosomatidae parasites as a promising target for designing new antiparasitic agents. *Curr. Top. Med Chem.* **21**, 1900–1921 (2021).
27. Verma, S., Mehta, A. & Shaha, C. CYP5122A1, a novel cytochrome P450 is essential for survival of Leishmania donovani. *PloS one* **6**, e25273 (2011).
28. Pandharkar, T. et al. Studies on the antileishmanial mechanism of action of the arylimidamide DB766: azole interactions and role of CYP5122A1. *Antimicrob. Agents Chemother.* **58**, 4682–4689 (2014).
29. Tulloch, L. B. et al. Sterol 14-alpha demethylase (CYP51) activity in Leishmania donovani is likely dependent upon cytochrome P450 reductase 1. *PLoS Pathog.* **20**, e1012382 (2024).
30. Lepesheva, G. I., Nes, W. D., Zhou, W., Hill, G. C. & Waterman, M. R. CYP51 from Trypanosoma brucei is obtusifoliol-specific. *Biochemistry* **43**, 10789–10799 (2004).
31. Lepesheva, G. I. et al. CYP51 from Trypanosoma cruzi: a phyla-specific residue in the B' helix defines substrate preferences of sterol 14alpha-demethylase. *J. Biol. Chem.* **281**, 3577–3585 (2006).
32. Schenkman, J. B. & Jansson, I. Spectral analyses of cytochromes P450. *Methods Mol. Biol.* **320**, 11–18 (2006).
33. Schenkman, J. B., Cinti, D. L., Orrenius, S., Moldeus, P. & Kraschnitz, R. The nature of the reverse type I (modified type II) spectral change in liver microsomes. *Biochemistry* **11**, 4243–4251 (1972).
34. Mast, N., Zheng, W., Stout, C. D. & Pikuleva, I. A. Binding of a cyano- and fluoro-containing drug bicalutamide to cytochrome P450 46A1: unusual features and spectral response. *J. Biol. Chem.* **288**, 4613–4624 (2013).
35. Fischer, R. T. et al. Lanosterol 14 alpha-methyl demethylase. Isolation and characterization of the third metabolically generated oxidative demethylation intermediate. *J. Biol. Chem.* **266**, 6124–6132 (1991).
36. Gottlieb, H. E., Kotlyar, V. & Nudelman, A. NMR Chemical Shifts of Common Laboratory Solvents as Trace Impurities. *J. Org. Chem.* **62**, 7512–7515 (1997).
37. Dacher, M. et al. Probing druggability and biological function of essential proteins in Leishmania combining facilitated null mutant and plasmid shuffle analyses. *Mol. Microbiol.* **93**, 146–166 (2014).
38. Valente, M., Castillo-Acosta, V. M., Vidal, A. E. & Gonzalez-Pacanowska, D. Overview of the role of kinetoplastid surface carbohydrates in infection and host cell invasion: prospects for therapeutic intervention. *Parasitology* **146**, 1743–1754 (2019).
39. Spath, G. F. et al. Lipophosphoglycan is a virulence factor distinct from related glycoconjugates in the protozoan parasite Leishmania major. *Proc. Natl Acad. Sci. USA* **97**, 9258–9263 (2000).
40. Borges, A. R., Link, F., Engstler, M. & Jones, N. G. The glycosylphosphatidylinositol anchor: a linchpin for cell surface versatility of trypanosomatids. *Front Cell Dev. Biol.* **9**, 720536 (2021).
41. Sacks, D. L. Metacyclogenesis in *Leishmania* promastigotes. *Exp. Parasitol.* **69**, 100–103 (1989).
42. Sacks, D. L., Brodin, T. N. & Turco, S. J. Developmental modification of the lipophosphoglycan from Leishmania major promastigotes during metacyclogenesis. *Mol. Biochem. Parasitol.* **42**, 225–233 (1990).

43. Coulson, R. M. & Smith, D. F. Isolation of genes showing increased or unique expression in the infective promastigotes of Leishmania major. *Mol. Biochem Parasitol.* **40**, 63–75 (1990).
44. Van Assche, T., Deschacht, M., da Luz, R. A., Maes, L. & Cos, P. Leishmania-macrophage interactions: insights into the redox biology. *Free Radic. Biol. Med.* **51**, 337–351 (2011).
45. Wang, M. Z. et al. Novel arylimidamides for treatment of visceral leishmaniasis. *Antimicrob. Agents Chemother.* **54**, 2507–2516 (2010).
46. Lee, A. K. et al. C-4 sterol demethylation enzymes distinguish bacterial and eukaryotic sterol synthesis. *Proc. Natl Acad. Sci. USA* **115**, 5884–5889 (2018).
47. He, M. et al. Mutations in the human SC4MOL gene encoding a methyl sterol oxidase cause psoriasiform dermatitis, microcephaly, and developmental delay. *J. Clin. Investig* **121**, 976–984 (2011).
48. Nes, W. D. Biosynthesis of cholesterol and other sterols. *Chem. Rev.* **111**, 6423–6451 (2011).
49. Ning Y. et al. Molecular Characterization of Sterol C4-Methyl Oxidase in Leishmania major. *Int J Mol Sci* **25**, 10908 (2024).
50. Cosentino, R. O. & Aguero, F. Genetic profiling of the isoprenoid and sterol biosynthesis pathway genes of Trypanosoma cruzi. *PLoS One* **9**, e96762 (2014).
51. Jones, N. G., Catta-Preta, C. M. C., Lima, A. & Mottram, J. C. Genetically Validated Drug Targets in Leishmania: Current Knowledge and Future Prospects. *ACS Infect. Dis.* **4**, 467–477 (2018).
52. Saunders, E. C. et al. Induction of a stringent metabolic response in intracellular stages of Leishmania mexicana leads to increased dependence on mitochondrial metabolism. *PLoS Pathog.* **10**, e1003888 (2014).
53. Jara, M. et al. Macromolecular biosynthetic parameters and metabolic profile in different life stages of Leishmania braziliensis: Amastigotes as a functionally less active stage. *PLoS One* **12**, e0180532 (2017).
54. Zhang, K. Balancing de novo synthesis and salvage of lipids by Leishmania amastigotes. *Curr. Opin. Microbiol* **63**, 98–103 (2021).
55. Mukherjee, S., Basu, S. & Zhang, K. Farnesyl pyrophosphate synthase is essential for the promastigote and amastigote stages in Leishmania major. *Mol. Biochem. Parasitol.* **230**, 8–15 (2019).
56. Moitra, S., Basu, S., Pawlowic, M., Hsu, F. F. & Zhang, K. De Novo Synthesis of Phosphatidylcholine Is Essential for the Promastigote But Not Amastigote Stage in Leishmania major. *Front Cell Infect. Microbiol* **11**, 647870 (2021).
57. Emami, S., Tavangar, P. & Keighobadi, M. An overview of azoles targeting sterol 14alpha-demethylase for antileishmanial therapy. *Eur. J. Med Chem.* **135**, 241–259 (2017).
58. La Rosa, C. et al. N-substituted-4-(pyridin-4-ylalkyl)piperazine-1-carboxamides and related compounds as Leishmania CYP51 and CYP5122A1 inhibitors. *Bioorg. Med Chem.* **113**, 117907 (2024).
59. Xu, X. & London, E. The effect of sterol structure on membrane lipid domains reveals how cholesterol can induce lipid domain formation. *Biochemistry* **39**, 843–849 (2000).
60. Xu, X. et al. Effect of the structure of natural sterols and sphingolipids on the formation of ordered sphingolipid/sterol domains (rafts). Comparison of cholesterol to plant, fungal, and disease-associated sterols and comparison of sphingomyelin, cerebrosides, and ceramide. *J. Biol. Chem.* **276**, 33540–33546 (2001).
61. Cournia, Z., Ullmann, G. M. & Smith, J. C. Differential effects of cholesterol, ergosterol and lanosterol on a dipalmitoyl phosphatidylcholine membrane: a molecular dynamics simulation study. *J. Phys. Chem. B* **111**, 1786–1801 (2007).
62. Hughes, A. L., Lee, C. Y., Bien, C. M. & Espenshade, P. J. 4-Methyl sterols regulate fission yeast SREBP-Scap under low oxygen and cell stress. *J. Biol. Chem.* **282**, 24388–24396 (2007).
63. Blosser, S. J., Merriman, B., Grahl, N., Chung, D. & Cramer, R. A. Two C4-sterol methyl oxidases (Erg25) catalyse ergosterol intermediate demethylation and impact environmental stress adaptation in Aspergillus fumigatus. *Microbiology* **160**, 2492–2506 (2014).
64. Doehl, J. S. et al. Leishmania HASP and SHERP genes are required for in vivo differentiation, parasite transmission and virulence attenuation in the host. *PLoS Pathog.* **13**, e1006130 (2017).
65. Sadlova, J. et al. The stage-regulated HASPB and SHERP proteins are essential for differentiation of the protozoan parasite Leishmania major in its sand fly vector, Phlebotomus papatasi. *Cell Microbiol* **12**, 1765–1779 (2010).
66. Knuepfer, E., Stierhof, Y. D., McKean, P. G. & Smith, D. F. Characterization of a differentially expressed protein that shows an unusual localization to intracellular membranes in Leishmania major. *Biochem J.* **356**, 335–344 (2001).
67. Moore, B. et al. Structural basis of molecular recognition of the Leishmania small hydrophilic endoplasmic reticulum-associated protein (SHERP) at membrane surfaces. *J. Biol. Chem.* **286**, 9246–9256 (2011).
68. Lepesheva, G. I. et al. Crystal structures of Trypanosoma brucei sterol 14alpha-demethylase and implications for selective treatment of human infections. *J. Biol. Chem.* **285**, 1773–1780 (2010).
69. Abdelhameed, A. et al. Synthesis and Antileishmanial Evaluation of Arylimidamide-Azole Hybrids Containing a Phenoxyalkyl Linker. *ACS Infect. Dis.* **7**, 1901–1922 (2021).
70. de Ibarra, A. A., Howard, J. G. & Snary, D. Monoclonal antibodies to Leishmania tropica major: specificities and antigen location. *Parasitology* **85**, 523–531 (1982).
71. Kapler, G. M., Coburn, C. M. & Beverley, S. M. Stable transfection of the human parasite Leishmania major delineates a 30-kilobase region sufficient for extrachromosomal replication and expression. *Mol. Cell Biol.* **10**, 1084–1094 (1990).
72. Murta, S. M., Vickers, T. J., Scott, D. A. & Beverley, S. M. Methylene tetrahydrofolate dehydrogenase/cyclohydrolase and the synthesis of 10-CHO-THF are essential in Leishmania major. *Mol. Microbiol.* **71**, 1386–1401 (2009).
73. Titus, R. G., Marchand, M., Boon, T. & Louis, J. A. A limiting dilution assay for quantifying Leishmania major in tissues of infected mice. *Parasite Immunol.* **7**, 545–555 (1985).
74. Livak, K. J. & Schmittgen, T. D. Analysis of relative gene expression data using real-time quantitative PCR and the 2(-Delta Delta C(T)) Method. *Methods* **25**, 402–408 (2001).
75. Ritz, C., Baty, F., Streibig, J. C. & Gerhard, D. Dose-response analysis using R. *PLoS One* **10**, e0146021 (2015).
76. Joice, A. C. et al. Antileishmanial Efficacy and Pharmacokinetics of DB766-Azole Combinations. *Antimicrob. Agents Chemother.* **62**, e01129–17 (2018).

Acknowledgements

This work was supported in part by the National Institute of Allergy and Infectious Diseases (NIAID) [R01AI139198 (M.Z.W.) and R15AI156746 (K.Z.)] and by the Centers of Biomedical Research Excellence (COBRE) funded by the National Institute of General Medical Sciences (NIGMS) [P30GM110761, P20GM113117, and P30GM145499] of the United States National Institutes of Health (NIH) and by the Office of the Assistant Secretary of Defense for Health Affairs under the Peer Reviewed Medical Research Program through award no. W81XWH-14-2-0017 (K.A.W.). Support for the NMR instrumentation was provided by an NIH Shared Instrumentation Grant (S10RR024664) and an NSF Major Research Instrumentation Award (1625923). Opinions, interpretations, conclusions, and recommendations are those of the authors and do not necessarily represent the official views of the NIH, the Department of Defense, or the U.S. Army. The authors would also like to acknowledge Prof. Harinantenaina L. Rakotondraibe,

Ph.D. (The Ohio State University) for his helpful comments regarding the NMR spectra presented in this manuscript.

Author contributions

Y.J., S.B., and M.F. performed the experimental studies, wrote parts of the manuscript, and contributed equally to the work. Y.N., I.M., A.M.J., L.Q., R.M., H.B., P.G., J.Q.W., S.W.S., and A.C.J. performed the experimental studies. J.L. carried out part of the analysis and interpretation. C.P., K.A.W., K.Z., and M.Z.W. designed the experiments, supervised the work, carried out the analysis and interpretation, wrote and revised the manuscript. M.Z.W. formulated the original idea.

Competing interests

The authors declare no competing interests.

Additional information

Supplementary information The online version contains supplementary material available at https://doi.org/10.1038/s41467-024-53790-5.

Correspondence and requests for materials should be addressed to Michael Zhuo Wang.

Peer review information *Nature Communications* thanks Michael Barrett and the other anonymous reviewer(s) for their contribution to the peer review of this work. A peer review file is available.

[1]Department of Pharmaceutical Chemistry, School of Pharmacy, The University of Kansas, Lawrence, KS 66047, USA. [2]Department of Biological Sciences, Texas Tech University, Lubbock, TX 79409, USA. [3]Synthetic Chemical Biology Core Laboratory, The University of Kansas, Lawrence, KS 66047, USA. [4]Division of Medicinal Chemistry and Pharmacognosy, College of Pharmacy, The Ohio State University, Columbus, OH 43210, USA. [5]College of Pharmacy, The Ohio State University, Columbus, OH 43210, USA. [6]Protein Production Group, The University of Kansas, Lawrence, KS 66047, USA. [7]Department of Pharmacy Practice, School of Pharmacy, The University of Kansas, Lawrence, KS 66047, USA. [8]These authors contributed equally: Yiru Jin, Somrita Basu, Mei Feng. ✉e-mail: michael.wang@ku.edu